

Gradient Algorithms for Complex Non-Gaussian Independent Component/Vector Extraction, Question of Convergence

Zbyněk Koldovský¹ and Petr Tichavský²

¹Acoustic Signal Analysis and Processing Group, Faculty of Mechatronics, Informatics, and
Interdisciplinary

Studies, Technical University of Liberec, Studentská 2, 461 17 Liberec, Czech Republic.

E-mail: zbynek.koldovsky@tul.cz, fax:+420-485-353112, tel:+420-485-353534

²The Czech Academy of Sciences, Institute of Information Theory and Automation,

Pod vodárenskou věží 4, P.O. Box 18, 182 08 Praha 8, Czech Republic. E-mail:

tichavsk@utia.cas.cz, fax:+420-2-868-90300, tel. +420-2-66052292

Abstract

We revise the problem of extracting one independent component from an instantaneous linear mixture of signals. The mixing matrix is parameterized by two vectors, one column of the mixing matrix and one row of the de-mixing matrix. The separation is based on the non-Gaussianity of the source of interest, while the other background signals are assumed to be Gaussian. Three gradient-based estimation algorithms are derived using the maximum likelihood principle and are compared with the Natural Gradient algorithm for Independent Component Analysis and with One-unit FastICA based on negentropy maximization. The ideas and algorithms are also generalized for the extraction of a vector component when the extraction proceeds jointly from a set of instantaneous mixtures. Throughout the paper, we address the problem of the size of the region of convergence for which the algorithms guarantee the extraction of the desired source. We show how that size is influenced by the ratio of powers of the sources within the mixture. Simulations confirm this observation where several algorithms are compared. They show various convergence behaviour in a scenario where the source of interest is dominant or weak. Here, our proposed modifications of the gradient methods taking into account the dominance/weakness of the source show improved global convergence property.

Index Terms

Blind Source Separation, Blind Source Extraction, Independent Component Analysis, Independent Vector Analysis

⁰Part of this paper was presented at the 25th European Signal Processing Conference (EUSIPCO 2017) in Kos, Greece. This work was supported by The Czech Science Foundation through Project No. 17-00902S.

I. INTRODUCTION

A. Independent Component Analysis

Independent Component Analysis has been a popular method studied for Blind Source Separation (BSS) since the 1990s [1], [2], [3], [4]. In the basic ICA model, signals observed on d sensors are assumed to be linear mixtures of d “original” signals, which are mutually independent in the statistical sense. The mixing model is given by

$$\mathbf{x}(n) = \mathbf{A}\mathbf{u}(n), \quad (1)$$

where $\mathbf{x}(n)$ is a $d \times 1$ vector of the mixed signals; \mathbf{A} is a $d \times d$ nonsingular mixing matrix; $\mathbf{u}(n)$ is a $d \times 1$ vector of the original signals; and n denotes the sample index. In the non-Gaussianity-based ICA, the j th original signal $u_j(n)$ (the j th element of $\mathbf{u}(n)$) is modeled as an independently and identically distributed (i.i.d.) sequence of random variables with the probability density function (pdf) $p_j(\cdot)$. The goal is to estimate \mathbf{A}^{-1} using $\mathbf{x}(n)$, $n = 1, \dots, N$, through finding a square de-mixing matrix \mathbf{W} such that $\mathbf{y}(n) = \mathbf{W}\mathbf{x}(n)$ are independent or as close to independent as possible. In the discussion that follows, we will omit the sample index n for the sake of brevity, except where it is required.

While our focus in this paper is on complex-valued signals and parameters, our conclusions are valid for the real-valued case as well.

B. Blind Extraction of One Independent Source

This work addresses the problem of extraction (separation) of one independent component, which is often sufficient in applications such as speaker source enhancement, passive radar and sonar, or in biomedical signal processing. The complete decomposition performed by ICA can be computationally very demanding and superfluous. This is especially remarkable when there is a large number of sensors (say, 10 or more), or when a large number of mixtures (say, 128 or more) are separated in parallel, as in the Frequency-Domain ICA (FD-ICA) [5]. The idea of extracting only one source can also be applied in joint BSS [6], [7], [8], especially in Independent Vector Analysis (IVA) [9]. Here, the “source” is represented by a vector of separated components from the mixtures that are mutually dependent (but independent of the other vector components).

BSS involves the permutation ambiguity [2], [10], and therefore some partial knowledge about the SOI must be available to determine which independent component is the one of our interest. For example, the a priori knowledge could be an expected direction of arrival (DOA) of the source, location of the source within a confined area [11], a property such as dominance within an angular range [12] or temporal structure [13], and so forth. Throughout this paper, we will assume that such knowledge is available in the form of an initial value of a (de)mixing parameter. The wanted signal will be referred to as *source of interest (SOI)* while the rest of the mixture will be referred to as *background*.

The theoretical part of this paper will be constrained to the determined case, which means that the background is assumed to be a mixture of $d - 1$ latent variables, or, in other words, the whole mixture obeys the determined mixing as in (1). This assumption need not be overly restrictive when only one source should be extracted. Indeed, when the mixture \mathbf{x} consists of more than d sources (underdetermined case), algorithms based on the

determined model can still be used provided that they are sufficiently robust against mismodeling and noise. However, these issues are beyond the scope of this paper.

C. State-of-the-Art

The blind separation of one particular non-Gaussian source has already been studied in several contexts and some authors refer to it as Blind Signal Extraction (BSE) [14], [15], [13]. Projection pursuit [16], a technique used for exploratory data analysis, aims at finding “interesting” projections, including 1-D signals. This “interestingness” is defined through various measures reflecting the distance of the projected signal’s pdf from the Gaussian distribution [2], [17]. Various criteria of the interestingness were also derived in other contexts. For example, kurtosis appears in methods for blind adaptive beamforming or as a higher-order cumulant-based contrast; see, e.g., [18], [19], [20].

This framework was unified under ICA based on information theory [21]. Namely, the independence of signals can be measured using mutual information, which is the Kullback-Leibler divergence between the joint density of signals and the product of their marginal densities. The signals are independent if and only if that mutual information equals zero. Provided that the elements of $\mathbf{y}(n)$ are not correlated, the mutual information of $\mathbf{y}(n)$ is equal to the sum of entropies of $y_1(n), \dots, y_d(n)$, up to a constant. Hence, it follows that an independent component can be sought through minimizing the entropy of the separated signal under the constraint $E[|\mathbf{w}^H \mathbf{x}|^2] = 1$; here $E[\cdot]$ stands for the expectation operator; and \mathbf{w}^H is a de-mixing vector (a row of the de-mixing matrix \mathbf{W}). The fact that entropy is a measure of non-Gaussianity reveals the connection between the ICA-based separation of one signal and the contrast-based BSE techniques [2], [22].

In fact, many ICA methods apply d BSE estimators sequentially [23] or in parallel [24] to find all independent components in the mixture. The orthogonal constraint, which requires that the sample correlation between separated signals is equal to zero, is imposed on the BSE outputs in order to prevent the algorithms from finding any components twice. For example, the well-known FastICA algorithm has three basic variants: One-Unit FastICA is a BSE method optimizing the component’s non-Gaussianity [25]; Deflation FastICA applies the one-unit version sequentially [26]; Symmetric FastICA runs d one-unit algorithms simultaneously [26], [27].

The separation accuracy of the above methods is known to be limited [28]. One-unit FastICA exploits only the non-Gaussianity of SOI and does not use the non-Gaussianity of the background [29]. The accuracy levels of deflation and symmetric FastICA are limited due to the orthogonal constraint [30]. While the latter limitation can be overcome, as shown, e.g., in [31], the limited accuracy of the one-unit approach poses an open problem, unless the BSE is done through the complete ICA. By comparing the performance analyses from [29], [32], [28] and the Cramér-Rao bound for ICA [31], it follows that one-unit methods can approach the optimum performance only when the background is Gaussian, but not otherwise.

D. Contribution

In this paper, we revisit the BSE problem by considering it explicitly as the goal to extract one component from the instantaneous mixture that is as close to being independent of the background as possible; we refer to this approach as *Independent Component Extraction (ICE)*. A re-parameterization of the mixing model is

introduced, in which the number of parameters is minimal for the BSE problem (the mixing and the separating vector related to the SOI). Then, a statistical model is adopted from ICA where the background is assumed to be jointly Gaussian. The classical maximum likelihood estimation of the mixing parameters is considered, by which simplistic gradient-based estimation algorithms are derived¹. The ICE approach provides a deeper insight into the BSE problem. In particular, it points to the role of the orthogonal constraint and to the fact that the constraint is inherently applied within One-Unit FastICA. The approach also reveals the role of the model of background's pdf.

It is worth pointing out here that a similar mixing and statistical model have been considered in methods that were designed for Cosmic Microwave Background extraction from the Wilkinson Microwave Anisotropy Probe (WMAP) data or from the more recent Planck Mission data [34]. However, there is one important difference that the mixing vector related to the SOI is assumed to be known. The methods are known under the name Internal Linear Combination (ILC) [?], [?]; see also [35].

For the practical output of this paper, we focus on the ability of BSE algorithms to ensure that the desired SOI is being extracted, not a different source². This is a crucial aspect in BSE, which has been little studied previously. When the extraction of the SOI is not guaranteed, it is necessary to extract all sources and to find the desired one afterwards, in which way the advantage of doing only one BSE task is lost. The other motivation is that the permutation ambiguity can impair on-line separation. For example, a sudden change of the region of convergence (ROC) due to dynamic signals and/or mixing conditions can cause that the current mixing vector estimate occurs within the ROC of a different source. Then, the given algorithm performs several "diverging" steps during which the separated sources are being permuted; the separation is poor in the meanwhile. Therefore, the size of the ROC to the SOI is studied. We point to the fact that the ROC is algorithm-dependent and is highly influenced by the so-called Scales Ratio (SR), which is the ratio of the powers of the SOI and the background. The experiments show that the ROC can depend on whether the optimization proceeds in the mixing or de-mixing parameters. Based on this, we propose novel variants of the gradient algorithms where the optimization parameters are selected automatically.

Next, the ideas are generalized to the extraction of a vector component, so-called *Independent Vector Extraction (IVE)*. Here, the problem defines several instantaneous mixtures to be treated simultaneously using joint statistical models. The goal is to extract one independent component per mixture where the extracted components should be as dependent as possible. IVE is an extension of ICE similar to that of ICA to IVA [36], [37]. A gradient algorithm with the automatic selection of the optimization parameters is derived, similarly to that for ICE. The experiments show that the convergence of the proposed IVE algorithm is superior to that for ICE because improved convergence within several mixtures has positive influence on the convergence within the other mixtures; the effect of the automatic selection is thus multiplied.

¹In this paper, an algorithm estimating the separating vector is introduced, compared to [33], where only the variant for the mixing vector estimation is described.

²We do not focus on the algorithms' accuracy as this is already a well-studied problem. The accuracy of BSE methods is fundamentally limited by the Cramér-Rao bound, which is asymptotically attainable, e.g., by One-Unit FastICA [28]; cf. the last paragraph of Section I-C; see also [?].

The rest of this paper is organized as follows. Section II introduces algebraic and statistical models for ICE. Section III is devoted to gradient-based ICE algorithms. The ideas and algorithms are generalized to the extraction of vector components in Section IV. Section V presents results of simulations, and Section VI concludes the paper.

II. INDEPENDENT COMPONENT EXTRACTION

Nomenclature: The following notation will be used throughout the article. Plain letters denote scalars, bold lower-case letters denote vectors, and bold capital letters denote matrices. The Matlab conventions for matrix/vector concatenation and indexing will be used, e.g., $[1; \mathbf{g}] = [1, \mathbf{g}^T]^T$, and $(\mathbf{A})_{j,:}$ is the j th row of \mathbf{A} . Next, \mathbf{g}^T , $\bar{\mathbf{g}}$, and \mathbf{g}^H denote the transpose, the complex conjugate value and the conjugate transpose of \mathbf{g} , respectively. Symbolic scalar and vector random variables will be denoted by lower-case letters, e.g., s and \mathbf{x} , while the quantities collecting their N samples will be denoted by bold (capital) letters, e.g., \mathbf{s} and \mathbf{X} . Estimated values of signals will be denoted by hats, e.g., $\hat{\mathbf{s}}$. For simplicity, the hat will be omitted in the case of estimated values of parameters, e.g., \mathbf{w} , unless it is necessary to distinguish between its estimated and true values.

A. Mixing Model Parameterization

Without any loss of generality, let the SOI be $s = u_1$ and \mathbf{a} be the first column of \mathbf{A} , so it can be partitioned as $\mathbf{A} = [\mathbf{a}, \mathbf{A}_2]$. Then, \mathbf{x} can be written in the form

$$\mathbf{x} = \mathbf{a}s + \mathbf{y}, \quad (2)$$

where $\mathbf{y} = \mathbf{A}_2\mathbf{u}_2$ and $\mathbf{u}_2 = [u_2, \dots, u_d]^T$. The single-target description (2) has been widely studied in array processing literature [38]. Here, the fact that $\mathbf{y} = \mathbf{A}_2\mathbf{u}_2$ means that we restrain our considerations to the determined scenario (the mixture consists of the same number of sources as that of the sensors).

Let the new mixing matrix for ICE and its inverse matrix be denoted by \mathbf{A}_{ICE} and \mathbf{W}_{ICE} , respectively. In ICE, the identification of \mathbf{A}_2 or the decomposition of \mathbf{y} into independent signals is *not* the goal. Therefore, the structure of the mixing matrix is $\mathbf{A}_{\text{ICE}} = [\mathbf{a}, \mathbf{Q}]$ where \mathbf{Q} is, for now, arbitrary.

Then, (2) can be written as

$$\mathbf{x} = \mathbf{A}_{\text{ICE}}\mathbf{v}, \quad (3)$$

where $\mathbf{v} = [s; \mathbf{z}]$, and $\mathbf{y} = \mathbf{Q}\mathbf{z}$. It holds that \mathbf{z} spans the same subspace as that spanned by \mathbf{u}_2 .

To complete the mixing model definition, we look at the inverse matrix $\mathbf{W}_{\text{ICE}} = \mathbf{A}_{\text{ICE}}^{-1}$. Let \mathbf{a} and \mathbf{W}_{ICE} be partitioned, respectively, as

$$\mathbf{a} = \begin{pmatrix} \gamma \\ \mathbf{g} \end{pmatrix} \quad (4)$$

and

$$\mathbf{W}_{\text{ICE}} = \begin{pmatrix} \mathbf{w}^H \\ \mathbf{B} \end{pmatrix}. \quad (5)$$

\mathbf{B} is required to be orthogonal to \mathbf{a} , i.e., $\mathbf{B}\mathbf{a} = \mathbf{0}$, which ensures that the signals separated by the lower part of \mathbf{W}_{ICE} , namely, by $\mathbf{B}\mathbf{x}$, do not contain any contribution of s . A useful selection is

$$\mathbf{B} = \begin{pmatrix} \mathbf{g} & -\gamma \mathbf{I}_{d-1} \end{pmatrix}, \quad (6)$$

where \mathbf{I}_d denotes the $d \times d$ identity matrix. Let \mathbf{w} be partitioned as

$$\mathbf{w} = \begin{pmatrix} \beta \\ \mathbf{h} \end{pmatrix}. \quad (7)$$

The de-mixing matrix then has the structure

$$\mathbf{W}_{\text{ICE}} = \begin{pmatrix} \mathbf{w}^H \\ \mathbf{B} \end{pmatrix} = \begin{pmatrix} \bar{\beta} & \mathbf{h}^H \\ \mathbf{g} & -\gamma \mathbf{I}_{d-1} \end{pmatrix}, \quad (8)$$

and from $\mathbf{A}_{\text{ICE}}^{-1} = \mathbf{W}_{\text{ICE}}$ it follows that

$$\mathbf{A}_{\text{ICE}} = \begin{pmatrix} \mathbf{a} & \mathbf{Q} \end{pmatrix} = \begin{pmatrix} \gamma & \mathbf{h}^H \\ \mathbf{g} & \frac{1}{\gamma} (\mathbf{g}\mathbf{h}^H - \mathbf{I}_{d-1}) \end{pmatrix}, \quad (9)$$

where β and γ are linked through

$$\bar{\beta}\gamma = 1 - \mathbf{h}^H \mathbf{g}. \quad (10)$$

The latter equation can also be written in the form $\mathbf{w}^H \mathbf{a} = 1$, which is known as the *distortionless response* constraint; see page 515 in [38]. The parameterization of the mixing and de-mixing matrix is similar to the one used in ILC [?], [35].

It is worth mentioning here that ICE and Multidimensional ICA [39] are similar to each other; the latter is also known as Independent Subspace Analysis (ISA) [40]. In ISA, the goal is to separate subspaces of components that are mutually independent while components inside of the subspaces can be dependent. The goal to separate one independent component thus could be formulated as a special case of ISA where \mathbf{u} is divided into two subspaces of dimensions 1 and $d - 1$, respectively. What makes ICE different is that the separation of the background subspace from the SOI is not as ambiguous as in ISA, which is ensured by the structure of the de-mixing matrix.

The free variables in the ICE mixing model are the elements of \mathbf{g} and \mathbf{h} , and one of the parameters β or γ . In total, there are $2d - 1$ free (real or complex) parameters. The role of \mathbf{a} , as follows from (2), is the *mixing vector* related to s , which is in beamforming literature also sometimes referred to as the steering vector. Next, \mathbf{w} is the *separating vector* as $s = \mathbf{w}^H \mathbf{x}$. For the background signal \mathbf{z} , it holds that

$$\mathbf{z} = \mathbf{B}\mathbf{x} = \mathbf{B}\mathbf{y} = \mathbf{B}\mathbf{A}_2 \mathbf{u}_2. \quad (11)$$

Note that \mathbf{A}_2 is not identified in the model, so the relationship between \mathbf{z} and \mathbf{u}_2 remains unknown after performing ICE. The components of \mathbf{z} are independent after the extraction only when $d = 2$ or, for $d > 2$, in very special cases that $\mathbf{B}\mathbf{A}_2 = \mathbf{\Lambda}\mathbf{P}$; $\mathbf{\Lambda}$ denotes a diagonal (scaling) matrix with non-zero elements on the main diagonal, and \mathbf{P} denotes a permutation matrix.

B. Indeterminacies

Similarly to ICA, the scales of s and of \mathbf{a} are ambiguous in the sense that, in (2) they can be replaced, respectively, by αs and $\alpha^{-1}\mathbf{a}$ where $\alpha \neq 0$. The scaling ambiguity can be avoided by fixing β or γ . A specific case occurs when $\gamma = 1$ [33], since then s corresponds to the so-called spatial image of the SOI on the first sensor [41], [42], [43]. This can be useful for modeling the pdf of s , as the physical meaning of that scale is often known. By contrast, when no such knowledge is given, it might be better to keep γ (or β) free.

The second ambiguity is that the role of $s = u_1$ is interchangeable with any independent component of \mathbf{x} , that is, with any u_i , $i = 2, \dots, d$. This fact is known as the permutation problem [22], [44] in BSS. As was already stated, in this work we assume that an initial guess of either \mathbf{a} or \mathbf{w} is given.

C. Statistical Model

The main principle of ICE is the same as that of ICA. We make the assumption that s and \mathbf{z} are *independent*, and ICE is formulated as follows:

Find vectors \mathbf{a} and \mathbf{w} such that $\mathbf{w}^T \mathbf{x}$ and $\mathbf{B}\mathbf{x}$ are independent (or as close to independent as possible).

Let the pdf of s and of \mathbf{z} be, respectively, denoted by $p_s(\xi_1)$ and $p_z(\boldsymbol{\xi}_2)$; ξ_1 and $\boldsymbol{\xi}_2$ denote free variables of appropriate dimensions. The joint pdf of s and \mathbf{z} is, owing to their mutual independence,

$$p_{\mathbf{s}}(\boldsymbol{\xi}) = p_s(\xi_1) \cdot p_z(\boldsymbol{\xi}_2), \quad (12)$$

where $\boldsymbol{\xi} = [\xi_1; \boldsymbol{\xi}_2]$. From (8), the joint pdf of the mixed signals $\mathbf{x} = \mathbf{A}_{\text{ICE}}\mathbf{v}$ is

$$p_{\mathbf{x}}(\boldsymbol{\xi}) = p_s(\mathbf{w}^H \boldsymbol{\xi}) \cdot p_z(\mathbf{B}\boldsymbol{\xi}) \cdot |\det \mathbf{W}_{\text{ICE}}|^2 \quad (13)$$

$$= p_s(\bar{\beta}\xi_1 + \mathbf{h}^H \boldsymbol{\xi}_2) \cdot p_z(\xi_1 \mathbf{g} - \gamma \boldsymbol{\xi}_2) \cdot |\gamma|^{2(d-2)}, \quad (14)$$

where the identity

$$\det \mathbf{W}_{\text{ICE}} = (-1)^{d-1} \gamma^{d-2} \quad (15)$$

$$= (-1)^{d-1} \beta^{-(d-2)} (1 - \mathbf{h}^H \mathbf{g})^{d-2}, \quad (16)$$

was used, which can easily be verified from (8) using (10).

The log-likelihood function of N signal samples depends on \mathbf{a} and \mathbf{w} ; hence it is

$$\mathcal{L}(\mathbf{a}, \mathbf{w}) = \frac{1}{N} \log \prod_{n=1}^N p_{\mathbf{x}}(\mathbf{a}, \mathbf{w} | \mathbf{x}(n)) \quad (17)$$

$$\begin{aligned} &= \frac{1}{N} \sum_{n=1}^N \log p_s(\mathbf{w}^H \mathbf{x}(n)) + \frac{1}{N} \sum_{n=1}^N \log p_z(\mathbf{B}\mathbf{x}(n)) \\ &+ (d-2) \log |\gamma|^2. \end{aligned} \quad (18)$$

D. Gaussian Background

As previously explained in Section II-A, the background signals are highly probable to remain unmixed after ICE, unless $d = 2$. This opens the problem of modeling the pdf of \mathbf{z} . A straightforward choice is that the components of \mathbf{z} have the circularly symmetric Gaussian distribution with zero mean and covariance \mathbf{C}_z , i.e.,

$\mathbf{z} \sim \mathcal{CN}(\mathbf{0}, \mathbf{C}_z)$. This choice can be justified by the fact that the said components are mixed and correlated; moreover, from the Central Limit Theorem it follows that their distribution is close to Gaussian [22]. The covariance matrix $\mathbf{C}_z = \mathbb{E}[\mathbf{z}\mathbf{z}^H]$ is a nuisance parameter.

In this paper, we restrain our considerations to this Gaussian background model, noting that other choices are worthy of future investigation. Hence, (18) takes the form

$$\begin{aligned} \mathcal{L}(\mathbf{a}, \mathbf{w}) = & \frac{1}{N} \sum_{n=1}^N \log p_s(\mathbf{w}^H \mathbf{x}(n)) - \frac{1}{N} \sum_{n=1}^N \mathbf{x}(n)^H \mathbf{B}^H \mathbf{C}_z^{-1} \mathbf{B} \mathbf{x}(n) + (d-2) \log |\gamma|^2 \\ & - \log \det \mathbf{C}_z - d \log \pi. \end{aligned} \quad (19)$$

E. Orthogonal Constraint

By inspecting (18) and (19), it can be seen that the link between \mathbf{a} and \mathbf{w} , which are both related to the SOI, is rather “weak”. Indeed, the first term on the right-hand side of (18) depends purely on \mathbf{w} , while the second and the third terms depend purely on \mathbf{a} . The only link between \mathbf{a} and \mathbf{w} is thus expressed in (10). Consequently, the log-likelihood function can have spurious maxima where \mathbf{a} and \mathbf{w} do not jointly correspond to the SOI.

Many ICA algorithms impose the orthogonal constraint (OG) [30], which decreases the number of unknown parameters in the mixing model. This constraint can be used to avoid spurious solutions in ICE and to stabilize the convergence of algorithms. Let now \mathbf{W}_{ICE} denote an ICE de-mixing matrix estimate and

$$\widehat{\mathbf{V}} = \begin{pmatrix} \widehat{\mathbf{s}} \\ \widehat{\mathbf{Z}} \end{pmatrix} = \mathbf{W}_{\text{ICE}} \mathbf{X} \quad (20)$$

be the estimated de-mixed signals, that is, $\widehat{\mathbf{s}}$ be the $1 \times N$ row vector of samples of the extracted SOI, and $\widehat{\mathbf{Z}}$ be the $(d-1) \times N$ matrix of samples of the background signals. The OG means that

$$\frac{1}{N} \widehat{\mathbf{s}} \cdot \widehat{\mathbf{Z}}^H = \frac{1}{N} \mathbf{w}^H \mathbf{X} \mathbf{X}^H \mathbf{B}^H = \mathbf{w}^H \widehat{\mathbf{C}}_x \mathbf{B}^H = \mathbf{0}, \quad (21)$$

where $\widehat{\mathbf{C}}_x = \mathbf{X} \mathbf{X}^H / N$ is the sample-based estimate of $\mathbf{C}_x = \mathbb{E}[\mathbf{x}\mathbf{x}^H]$.

The OG introduces a link between \mathbf{a} and \mathbf{w} , so \mathbf{W}_{ICE} is a function of either \mathbf{a} or \mathbf{w} . The dependencies, whose derivations are given in Appendix A, are

$$\mathbf{w} = \frac{\widehat{\mathbf{C}}_x^{-1} \mathbf{a}}{\mathbf{a}^H \widehat{\mathbf{C}}_x^{-1} \mathbf{a}}, \quad (22)$$

when \mathbf{a} is the dependent variable, and

$$\mathbf{a} = \frac{\widehat{\mathbf{C}}_x \mathbf{w}}{\mathbf{w}^H \widehat{\mathbf{C}}_x \mathbf{w}}, \quad (23)$$

when the dependent variable is \mathbf{w} .

Interestingly, the coupling (22) corresponds to the approximation of

$$\mathbf{w}_{\text{MPDR}}^H \mathbf{x} = \frac{\mathbf{a}^H \mathbf{C}_x^{-1}}{\mathbf{a}^H \mathbf{C}_x^{-1} \mathbf{a}} \mathbf{x}, \quad (24)$$

which is the minimum-power distortionless (MPDR) beamformer steered in the direction given by \mathbf{a} , the well-known optimum beamformer in array processing theory [38]; see also [33]. In Appendix B, it is shown that if \mathbf{a} is equal to its true value, then

$$\mathbf{w}_{\text{MPDR}}^H \mathbf{x} = s. \quad (25)$$

The advantage of (23) is that the computation of \mathbf{a} does not involve the inverse of $\widehat{\mathbf{C}}_{\mathbf{x}}$.

III. GRADIENT-BASED ICE ALGORITHMS

In this section, we derive gradient ICE algorithms aiming at the maximum likelihood estimation through searching for the maximum of (19). Since p_s and $\mathbf{C}_{\mathbf{z}}$ in (19) are not known, we propose a contrast function replacing the true one where p_s and $\mathbf{C}_{\mathbf{z}}$ are approximated in a certain way. This is sometimes referred to as the quasi-maximum likelihood approach; see, e.g., [45].

A. Optimization in \mathbf{w}

For the optimization in \mathbf{w} , given the coupling (23), β is selected as a free variable while γ is dependent. Following (19), the contrast function is defined as

$$\mathcal{C}(\mathbf{a}, \mathbf{w}) = \frac{1}{N} \sum_{n=1}^N \left\{ \log f(\mathbf{w}^H \mathbf{x}(n)) - \mathbf{x}(n)^H \mathbf{B}^H \mathbf{R} \mathbf{B} \mathbf{x}(n) \right\} + (d-2) \log |\gamma|^2, \quad (26)$$

where $f(\cdot)$ is the model pdf of the target signal (replacing p_s), and \mathbf{R} is a weighting positive definite matrix (replacing $\mathbf{C}_{\mathbf{z}}^{-1}$).

Using the Wirtinger calculus [46], [47], we derive in Appendix C that the gradient of \mathcal{C} with respect to \mathbf{w}^H , under the coupling (23), equals

$$\begin{aligned} \left. \frac{\partial \mathcal{C}}{\partial \mathbf{w}^H} \right|_{\text{w.r.t. (23)}} &= -\frac{1}{N} \mathbf{X} \phi(\mathbf{w}^H \mathbf{X})^T + 2\mathbf{a} \operatorname{tr}(\mathbf{R} \widehat{\mathbf{C}}_{\mathbf{z}}) - (\mathbf{w}^H \widehat{\mathbf{C}}_{\mathbf{x}} \mathbf{w})^{-1} (\widehat{\mathbf{C}}_{\mathbf{x}} \mathbf{E}^H \mathbf{R} \widehat{\mathbf{C}}_{\mathbf{z}} \mathbf{h} - \operatorname{tr}(\mathbf{R} \mathbf{B} \widehat{\mathbf{C}}_{\mathbf{x}} \mathbf{E}^H) \widehat{\mathbf{C}}_{\mathbf{x}} \mathbf{e}_1) \\ &\quad - 2(d-2)\mathbf{a} + \bar{\gamma}^{-1} (d-2) (\mathbf{w}^H \widehat{\mathbf{C}}_{\mathbf{x}} \mathbf{w})^{-1} \widehat{\mathbf{C}}_{\mathbf{x}} \mathbf{e}_1, \end{aligned} \quad (27)$$

where $\operatorname{tr}(\cdot)$ denotes the trace; $\mathbf{E} = [\mathbf{0} \quad \mathbf{I}_{d-1}]$; \mathbf{e}_1 denotes the first column of \mathbf{I}_d ; and

$$\phi(\xi) = -\frac{\partial \log f(\xi)}{\partial \xi} \quad (28)$$

is the score function of the model pdf $f(\cdot)$.

Now, we put $\mathbf{R} = \widehat{\mathbf{C}}_{\mathbf{z}}^{-1}$; this is a choice for which the derivative of (19) with respect to the unknown

parameter \mathbf{C}_z is equal to zero. Then, the following identities can be applied in (27).

$$\text{tr}(\widehat{\mathbf{C}}_z^{-1}\widehat{\mathbf{C}}_z) = \text{tr}(\mathbf{I}_{d-1}) = d - 1, \quad (29)$$

$$\mathbf{E}^H \mathbf{h} + \beta \mathbf{e}_1 = \mathbf{w}, \quad (30)$$

$$\begin{aligned} \widehat{\mathbf{C}}_z^{-1} \mathbf{B} \widehat{\mathbf{C}}_x &= \widehat{\mathbf{C}}_z^{-1} \mathbf{B} \mathbf{X} \mathbf{X}^H / N \\ &= \widehat{\mathbf{C}}_z^{-1} \widehat{\mathbf{Z}} [\widehat{\mathbf{s}}^H \quad \widehat{\mathbf{Z}}^H] \mathbf{A}_{\text{ICE}}^H = \mathbf{E} \mathbf{A}_{\text{ICE}}^H \end{aligned} \quad (31)$$

$$\begin{aligned} \text{tr}(\widehat{\mathbf{C}}_z^{-1} \mathbf{B} \widehat{\mathbf{C}}_x \mathbf{E}^H) &= \text{tr}(\mathbf{E} \mathbf{A}_{\text{ICE}}^H \mathbf{E}^H) = \\ &= \bar{\gamma}^{-1} \text{tr}(\mathbf{h} \mathbf{g}^H - \mathbf{I}_{d-1}) = \\ &= -\beta - (d-2) \bar{\gamma}^{-1}, \end{aligned} \quad (32)$$

where we used (20) and (21); (27) is now simplified to

$$\left. \frac{\partial \mathcal{C}}{\partial \mathbf{w}^H} \right|_{\text{w.r.t. (23)}} = \mathbf{a} - \frac{1}{N} \mathbf{X} \phi(\mathbf{w}^H \mathbf{X})^T. \quad (33)$$

In fact, $\mathbf{R} = \widehat{\mathbf{C}}_z^{-1}$ depends on the current value of \mathbf{w} since $\widehat{\mathbf{C}}_z = \mathbf{B} \widehat{\mathbf{C}}_x \mathbf{B}^H$. It means that, with any estimate of \mathbf{w} , the distribution of $\widehat{\mathbf{Z}} = \mathbf{B} \mathbf{X}$ is assumed to be $\mathcal{CN}(\mathbf{0}, \widehat{\mathbf{C}}_z)$, which obviously introduces little (or no) information into the contrast function. $\widehat{\mathbf{C}}_z$ is close to the true covariance \mathbf{C}_z only when \mathbf{a} is close to its true value.

For $N \rightarrow +\infty$, (33) takes on the form

$$\frac{\partial \mathcal{C}}{\partial \mathbf{w}^H} = \mathbf{a} - \mathbb{E}[\mathbf{x} \phi(\mathbf{w}^H \mathbf{x})]. \quad (34)$$

When \mathbf{w} is the ideal separating vector, that is, when $\mathbf{w}^H \mathbf{x} = s$, then from (2) it follows that

$$\frac{\partial \mathcal{C}}{\partial \mathbf{w}^H} = (1 - \mathbb{E}[s \phi(s)]) \mathbf{a}. \quad (35)$$

This shows us that the true separating vector is a stationary point of the contrast function only if $\phi(\cdot)$ satisfies the condition

$$\mathbb{E}[s \phi(s)] = 1. \quad (36)$$

Based on this observation, we propose a method whose steps are described in Algorithm 1. In every step, it iterates in the direction of the steepest ascent of \mathcal{C} where $\mathbf{R} = \widehat{\mathbf{C}}_z^{-1}$ (step 9), and $\phi(\cdot)$ is normalized so that condition (36) is satisfied for the current target signal estimate $\widehat{s} = \mathbf{w}^H \mathbf{x}$, that is, $\phi(\widehat{s}) \leftarrow \phi(\widehat{s}) / (\widehat{s} \phi(\widehat{s})^T / N)$ (see steps 7 and 8). This is repeated until the norm of the gradient is smaller than tol ; μ is the step length parameter; and \mathbf{w}_{ini} is the initial guess. We call this method OGICE $_{\mathbf{w}}$.

In fact, (34) coincides with the gradient of a heuristic criterion derived from mutual information in [32] (page 870, Eq. 4). The author, D.-T. Pham, called this approach ‘‘Blind Partial Separation’’. Our derivation provides a deeper insight into this result by showing its connection with maximum likelihood estimation. Most importantly, it is seen that (33) follows from a particular parameterization of the (de)-mixing model, it imposes the OG between \mathbf{a} and \mathbf{w} , and it relies on the Gaussian modeling of the background signals whose covariance is estimated as $\widehat{\mathbf{C}}_z$.

Algorithm 1: OGICE_w: separating vector estimation based on orthogonally constrained gradient-ascent algorithm

Input: \mathbf{X} , \mathbf{w}_{ini} , μ , tol

Output: \mathbf{a} , \mathbf{w}

```

1  $\hat{\mathbf{C}}_{\mathbf{x}} = \mathbf{X}\mathbf{X}^H/N$ ;
2  $\mathbf{w} = \mathbf{w}_{\text{ini}}$ ;
3 repeat
4    $\lambda_{\mathbf{w}} \leftarrow (\mathbf{w}^H \hat{\mathbf{C}}_{\mathbf{x}} \mathbf{w})^{-1}$ ;
5    $\mathbf{a} \leftarrow \lambda_{\mathbf{w}} \hat{\mathbf{C}}_{\mathbf{x}} \mathbf{w}$ ;           /* OG constraint (23) */
6    $\hat{\mathbf{s}} \leftarrow \mathbf{w}^H \mathbf{X}$ ;
7    $\nu \leftarrow \hat{\mathbf{s}} \phi(\hat{\mathbf{s}})^T / N$ ;       /* due to cond. (36) */
8    $\Delta \leftarrow \mathbf{a} - \nu^{-1} \mathbf{X} \phi(\hat{\mathbf{s}})^T / N$ ;           /* by (33) */
9    $\mathbf{w} \leftarrow \mathbf{w} + \mu \Delta$ ;       /* gradient ascent */
10 until  $\|\Delta\| < \text{tol}$ ;
```

B. Optimization in \mathbf{a}

The gradient with respect to \mathbf{a} when \mathbf{w} is dependent through (22) and when $\gamma = 1$ has been derived in [33]. Treating γ as a free variable, and by putting $\mathbf{R} = \hat{\mathbf{C}}_{\mathbf{z}}^{-1}$, the gradient reads

$$\left. \frac{\partial \mathcal{C}}{\partial \mathbf{a}^H} \right|_{\text{w.r.t. (22)}} = \mathbf{w} - \frac{\lambda_{\mathbf{a}}}{N} \hat{\mathbf{C}}_{\mathbf{x}}^{-1} \mathbf{X} \phi(\mathbf{w}^H \mathbf{X})^T, \quad (37)$$

where $\lambda_{\mathbf{a}} = (\mathbf{a}^H \hat{\mathbf{C}}_{\mathbf{x}}^{-1} \mathbf{a})^{-1}$. For $N \rightarrow +\infty$, the true mixing vector is a stationary point only if (36) is fulfilled. The corresponding algorithm, similar to that proposed in [33] but leaving γ free, will be referred to as OGICE_a.

C. Preconditioning

The multiplicative form of the mixing model (3) allows us to consider the gradient computed according to transformed input signals $\mathbf{U} = \mathbf{D}\mathbf{X}$, where \mathbf{D} is a *preconditioning* non-singular matrix. We will consider the preconditioning applied within OGICE_w since this will help us to reveal the connection between OGICE_w and three well-known ICA/BSE algorithms.

Let $\mathbf{w}_{\mathbf{x}}$ and $\mathbf{w}_{\mathbf{u}}$ be the separating vectors operating on \mathbf{X} and \mathbf{U} , respectively, giving the same extracted signal, i.e., $\hat{\mathbf{s}} = \mathbf{w}_{\mathbf{x}}^H \mathbf{X} = \mathbf{w}_{\mathbf{u}}^H \mathbf{U}$. It follows that $\mathbf{w}_{\mathbf{x}} = \mathbf{D}^H \mathbf{w}_{\mathbf{u}}$. Consider now the gradient (33) when the input data are \mathbf{U} and the initial vector is $\mathbf{w}_{\mathbf{u}}$, which will be denoted by $\Delta_{\mathbf{u}}$. The sample covariance matrix of \mathbf{U} is $\hat{\mathbf{C}}_{\mathbf{u}} = \mathbf{D} \hat{\mathbf{C}}_{\mathbf{x}} \mathbf{D}^H$, so the right-hand side of (33) gives

$$\Delta_{\mathbf{u}} = \frac{\hat{\mathbf{C}}_{\mathbf{u}} \mathbf{w}_{\mathbf{u}}}{\mathbf{w}_{\mathbf{u}}^H \hat{\mathbf{C}}_{\mathbf{u}} \mathbf{w}_{\mathbf{u}}} - \frac{1}{N} \mathbf{U} \phi(\hat{\mathbf{s}})^T = \frac{\mathbf{D} \hat{\mathbf{C}}_{\mathbf{x}} \mathbf{D}^H \mathbf{w}_{\mathbf{u}}}{\mathbf{w}_{\mathbf{u}}^H \mathbf{D} \hat{\mathbf{C}}_{\mathbf{x}} \mathbf{D}^H \mathbf{w}_{\mathbf{u}}} - \frac{1}{N} \mathbf{D} \mathbf{X} \phi(\hat{\mathbf{s}})^T = \mathbf{D} \left(\frac{\hat{\mathbf{C}}_{\mathbf{x}} \mathbf{w}_{\mathbf{x}}}{\mathbf{w}_{\mathbf{x}}^H \hat{\mathbf{C}}_{\mathbf{x}} \mathbf{w}_{\mathbf{x}}} - \frac{1}{N} \mathbf{X} \phi(\hat{\mathbf{s}})^T \right) = \mathbf{D} \Delta_{\mathbf{x}}, \quad (38)$$

where $\Delta_{\mathbf{x}}$ denotes the ‘‘normal’’ gradient, that is, when the input data are \mathbf{X} and the initial vector is $\mathbf{w}_{\mathbf{x}}$. Note that (38) remains valid when the normalization of ϕ (dividing by ν) is taken into account, because ν is only a function of \hat{s} .

After $\mathbf{w}_{\mathbf{u}}$ is updated as $\mathbf{w}_{\mathbf{u}}^{\text{new}} = \mathbf{w}_{\mathbf{u}} + \mu\Delta_{\mathbf{u}}$, the extracted signal is equal to

$$(\mathbf{w}_{\mathbf{u}}^{\text{new}})^H \mathbf{U} = (\mathbf{w}_{\mathbf{u}} + \mu\Delta_{\mathbf{u}})^H \mathbf{U} = (\mathbf{D}^{-H} \mathbf{w}_{\mathbf{x}} + \mu \mathbf{D} \Delta_{\mathbf{x}})^H \mathbf{D} \mathbf{X} = (\mathbf{w}_{\mathbf{x}} + \mu \mathbf{D}^H \mathbf{D} \Delta_{\mathbf{x}})^H \mathbf{X}. \quad (39)$$

It follows that the gradient update computed on the preconditioned data \mathbf{U} corresponds with a modified update rule for $\mathbf{w}_{\mathbf{x}}$ given by

$$\mathbf{w}_{\mathbf{x}} \leftarrow \mathbf{w}_{\mathbf{x}} + \mu \mathbf{D}^H \mathbf{D} \Delta_{\mathbf{x}}. \quad (40)$$

For $\mathbf{D} = \mathbf{I}_d$, the modified update rule obviously coincides with the original one. In the following subsection, we will consider other special choices of \mathbf{D} and compare the modified $\text{OGICE}_{\mathbf{w}}$ with other ICA/BSE methods known in the literature.

D. Relation to gradient and natural gradient ICA methods

Here, $\text{OGICE}_{\mathbf{w}}$ is compared with the method by Bell and Sejnowski [48] for ICA and with its popular modification known as Amari’s Natural Gradient (NG) algorithm [49]; see also [50] and [47] for the complex-valued variant. In each step of the Bell and Sejnowski’s method (BS), the whole de-mixing matrix is updated as

$$\Delta \mathbf{W} \leftarrow \mathbf{W}^{-H} - \overline{\phi(\mathbf{W}\mathbf{X})} \mathbf{X}^H / N. \quad (41)$$

After taking the conjugate transpose on both sides, and denoting $\mathbf{W}^{-1} = \mathbf{A}$, this update can be re-written as

$$\Delta \mathbf{W}^H \leftarrow \mathbf{A} - \mathbf{X} \phi(\mathbf{W}\mathbf{X})^T / N. \quad (42)$$

Now, the right-hand side of (33) corresponds to any row on the right-hand side of (42).

The de-mixing matrix update in NG is obtained when the right-hand side of (42) is multiplied by $\mathbf{W}^H \mathbf{W}$ from left, which gives

$$\Delta \mathbf{W}^H \leftarrow \mathbf{W}^H (\mathbf{I}_d - \mathbf{W}\mathbf{X} \phi(\mathbf{W}\mathbf{X})^T / N). \quad (43)$$

$\text{OGICE}_{\mathbf{w}}$ becomes similar to NG when considering it with the modified update (40) where the precondition matrix $\mathbf{D} = \mathbf{W}_{\text{ICE}}$. This choice corresponds to the update when the input data are pre-separated by the current de-mixing matrix prior to each iteration, and the starting \mathbf{w} is equal to the unit vector (the first column of \mathbf{I}_d).

The main difference between $\text{OGICE}_{\mathbf{w}}$ and the respective ICA algorithms thus resides in that BS and NG perform updates of the whole de-mixing matrix, while $\text{OGICE}_{\mathbf{w}}$ updates only its first row (the separating vector) under the orthogonal constraint. Next, the nonlinearity in $\text{OGICE}_{\mathbf{w}}$ is normalized according to (36), while neither BS nor NG apply any normalization.

E. Relation to One-unit FastICA

One-unit FastICA (FICA) was derived as a fixed-point algorithm that minimizes the entropy of the extracted signal under the unit scale constraint. The FICA update for the separating vector can be written as [25]

$$\mathbf{w} \leftarrow \mathbf{w} - (\widehat{\mathbf{C}}_{\mathbf{x}}^{-1} \mathbf{X} \psi(\widehat{\mathbf{s}})^T / N - \nu \mathbf{w}) / (\rho - \nu), \quad (44)$$

$$\mathbf{w} \leftarrow \mathbf{w} / \sqrt{\mathbf{w}^H \widehat{\mathbf{C}}_{\mathbf{x}} \mathbf{w}}, \quad (45)$$

where $\nu = \widehat{\mathbf{s}} \psi(\widehat{\mathbf{s}})^T / N$ and $\rho = \psi'(\widehat{\mathbf{s}}) \mathbf{1}_N / N$, where ψ' is the derivative of ψ , and $\mathbf{1}_N$ denotes the column vector of ones of length N . Note that (45) corresponds to the normalization of \mathbf{w} so that the scale of the extracted signal is one.

FICA is more known when it operates on pre-whitened data \mathbf{X} , which means that they are normalized prior to the optimization so that their sample covariance matrix is \mathbf{I}_d . This corresponds with the choice of the preconditioning matrix in Section III-C as $\mathbf{D} = \mathbf{F} \widehat{\mathbf{C}}_{\mathbf{x}}^{-1/2}$, where $\widehat{\mathbf{C}}_{\mathbf{x}}^{-1/2}$ denotes the inverse matrix square root of $\widehat{\mathbf{C}}_{\mathbf{x}}$, and \mathbf{F} is an arbitrary unitary matrix. Then, it holds that $\mathbf{D}^H \mathbf{D} = \widehat{\mathbf{C}}_{\mathbf{x}}^{-1}$, and we can compare the modified update rule of OGICE_w with (44). Specifically, the OGICE_w update modified according to (40) together with the nonlinearity normalization can be written as

$$\mathbf{w} \leftarrow \mathbf{w} + \mu \left(\frac{\mathbf{w}}{\mathbf{w}^H \widehat{\mathbf{C}}_{\mathbf{x}} \mathbf{w}} - \nu^{-1} \frac{1}{N} \widehat{\mathbf{C}}_{\mathbf{x}}^{-1} \mathbf{X} \phi(\widehat{\mathbf{s}})^T \right) \quad (46)$$

where μ is the step length parameter. By comparing (44) and (46), the updates coincide when $\mu = \frac{\nu}{\rho - \nu}$ provided that $\mathbf{w}^H \widehat{\mathbf{C}}_{\mathbf{x}} \mathbf{w} = 1$.

In conclusion, FICA and OGICE_w correspond to the same method when (a) the input data are pre-whitened (directly or through the preconditioning matrix and the modified update), (b) the step length in OGICE_w is selected adaptively as $\mu = \frac{\nu}{\rho - \nu}$, and (c) OGICE_w is forced to operate on the unit-scale sphere, which can be achieved through normalizing \mathbf{w} after each iteration as in (45). These results extend the analysis done in [?].

F. Switched optimization

When all sources should be separated, as in ICA, it is less important which source is extracted in which output channel as all sources are finally separated. However, when only one source should be extracted (based on the initial value of the mixing/separating vector), the size of the region of convergence (ROC) to the SOI becomes essential.

The ROC depends on the surface of the objective function of the given algorithm. This is influenced by all properties of the observed signals, namely, by the signals' distributions and by the initial Signal-to-Interference Ratio (SIR), where the latter is a function of the signals' scales and of the mixing matrix. The influence of the initial SIR is, however, difficult to analyze as it is different on each input channel.

Nevertheless, we can constrain our considerations to situations where the initial SIR is approximately the same on all channels. This happens, for example, when mutual distances of sensors are small compared to the distances of the sources from the sensor array. Then, we can assume that the magnitude of each element of the mixing matrix is approximately equal to a constant, so the initial SIRs are mainly influenced by the scales of

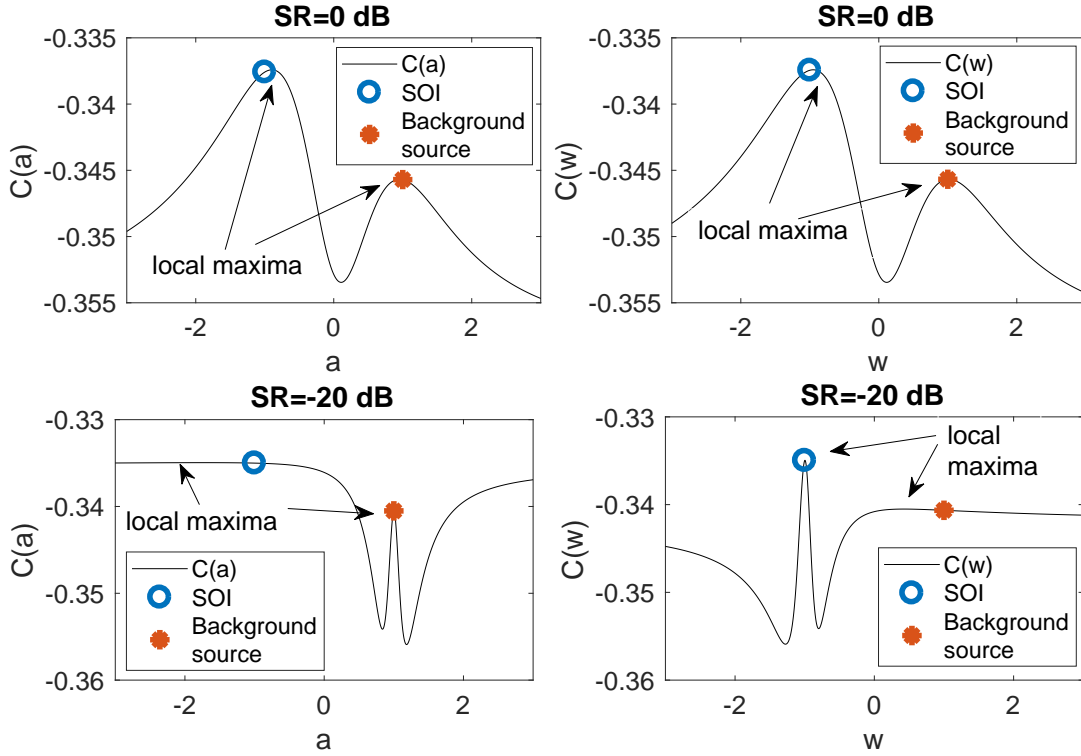


Fig. 1. Examples of the contrast function (26) as it depends on $\mathbf{a} = [1; a]$ and $\mathbf{w} = [1; w]$, respectively, when SR is 0 dB and -20 dB.

the sources. Let us define Scales Ratio (SR) related to the SOI as

$$\text{SR} = \frac{\text{E}[|s|^2]}{\frac{1}{d-1} \sum_{i=2}^d \text{E}[|u_i|^2]}. \quad (47)$$

The following example shows how the ROC of the OGICE algorithms can be influenced by SR.

Consider a situation where the SOI is a “weak” signal, i.e., $\text{SR} \ll 0$ dB. The mixing vector \mathbf{a} is then “hard” to find while the background subspace can be identified “easily”. For the de-mixing matrix, the problem is reciprocal. The estimation of \mathbf{B} in (8) is inaccurate as \mathbf{B} depends purely on \mathbf{a} , while the estimation of \mathbf{w} yields a low variance.

Fig. 1 shows an objective function in the case of a real-valued mixture of two Laplacean components where one plays the role of the SOI and the other one is the background source (but the roles can be interchanged); the number of samples is $N = 1000$; the mixing matrix is $\mathbf{A} = \begin{pmatrix} 1 & 1 \\ -1 & 1 \end{pmatrix}$; SR is considered in two settings: 0 dB and -20 dB, respectively. The function (26) is shown as it depends on a and w , respectively, where the mixing vector is $\mathbf{a} = [1; a]$ and the separating vector is $\mathbf{w} = [1; w]$, respectively. The nonlinearity is $\log f(x) = -\log |\cosh(x/\sigma_x)|$ where σ_x^2 is the variance of the input. The perfect extraction of the SOI is achieved for $a = -1$ and $w = -1$, while $a = 1$ and $w = 1$ correspond to the extraction of the background source.

For $\text{SR} = 0$ dB, the surface of the contrast function as it depends on a or w , respectively, is almost the same. The local maxima are slightly biased from perfect solutions, and the sizes of ROC related to the maxima are approximately equal for both sources.

For $SR = -20$ dB, the background source dominates the mixture. Here, the maximum corresponding to the mixing vector of the SOI is significantly biased from its ideal value, the function is almost flat in the vicinity of that maximum, and the corresponding ROC is wide. By contrast, the separating vector for SOI is precisely localized by a sharp local maximum, which has a narrow ROC. The exact opposite is true for the maxima corresponding to the dominating background source.

In this example, $OGICE_w$ is more advantageous when $SR_{in} \gg 0$ dB in the sense that the ROC corresponding to the SOI is wide. Even when the initialization of $OGICE_w$ is significantly deviated, the probability of the successful convergence is high. Similarly, $OGICE_a$ is advantageous when $SIR_{in} \ll 0$ dB. However, it is worth emphasizing that these properties of the algorithms depend on the mixing matrix, hence, also on the choice of the preconditioning matrix introduced in Section III-C. For example, $OGICE_w$ with the modified update (40) is advantageous in the example here when $\mathbf{D} = \mathbf{I}_d$.

The above observations suggest that partial knowledge of mixing conditions can be used towards successful extraction of the SOI. In a purely blind scenario, SR is not known. We therefore propose the following heuristic approach for the selection between the optimization in \mathbf{a} and \mathbf{w} . Let \mathbf{a} be the current estimate of the mixing vector. Then,

$$\mathbf{b} = \hat{\mathbf{C}}_x \mathbf{a} \quad (48)$$

can be viewed as an approximate eigenvector of $\hat{\mathbf{C}}_x$ corresponding to the largest eigenvalue, which is approximately equal to $\lambda_b = b_1/a_1$. Thus, $\|\mathbf{a}/a_1 - \mathbf{b}/\lambda_b\|$ is small when \mathbf{a} is close to the dominant eigenvector.

Next, to assess the dominance of that eigenvector, that is, whether it is significantly larger compared to the other eigenvectors, we propose to compute the ratio of norms of matrices $\hat{\mathbf{C}}_x - \lambda_b \mathbf{b} \mathbf{b}^H / \|\mathbf{b}\|^2$ and $\hat{\mathbf{C}}_x$. The ratio is small when \mathbf{b} is a dominant eigenvector of $\hat{\mathbf{C}}_x$. The criterion of ‘‘proximity and dominance’’ is therefore defined as

$$\mathcal{B}(\mathbf{a}) = \|\mathbf{a}/a_1 - \mathbf{b}/\lambda_b\| \frac{\|\hat{\mathbf{C}}_x - \lambda_b \mathbf{b} \mathbf{b}^H / \|\mathbf{b}\|^2\|_F}{\|\hat{\mathbf{C}}_x\|_F}. \quad (49)$$

The proposed algorithm, referred to as $OGICE_s$, selects the optimization parameter based on the current value of $\mathcal{B}(\mathbf{a})$. When $\mathcal{B}(\mathbf{a}) < \tau$, the optimization in \mathbf{w} is selected; otherwise, the optimization proceeds in \mathbf{a} . Normally, we select $\tau = 0.1$. To lower the computational load, the criterion is recomputed only once after Q iterations ($Q = 10$). The stopping condition of $OGICE_s$ is the same as that in $OGICE_w$ or $OGICE_a$; see the summary in Algorithm 2.

IV. INDEPENDENT VECTOR EXTRACTION

A. Definition

In this section, we extend the ideas in previous sections, which were derived for a single mixture, for joint extraction of an independent vector component from a set of K instantaneous mixtures (each of the same dimension d)

$$\mathbf{x}^k = \mathbf{A}_{ICE}^k \mathbf{v}^k, \quad k = 1, \dots, K. \quad (50)$$

Here, \mathbf{A}_{ICE}^k obeys the same structure as (3), and $\mathbf{v}^k = [s^k; \mathbf{z}^k]$. A joint mixture model can be written as

$$\mathbf{x} = \mathbb{A}_{IVE} \mathbf{v}. \quad (51)$$

Algorithm 2: OGICE_s: ICE algorithm with automatic selection of optimization parameter

Input: \mathbf{X} , \mathbf{a}_{ini} , μ , tol , Q
Output: \mathbf{a} , \mathbf{w}

```

1  $\hat{\mathbf{C}}_{\mathbf{x}} = \mathbf{X}\mathbf{X}^H/N$ ;  $\mathbf{a} = \mathbf{a}_{\text{ini}}$ ;  $i = 0$ ;
2 repeat
3   if  $i \equiv 0 \pmod{Q}$  then
4     |  $\kappa = \mathcal{B}(\mathbf{a})$ ; /* using (49) */
5     end
6      $i \leftarrow i + 1$ ;
7     if  $\kappa < 0.1$  then
8       | Update  $\mathbf{w}$  as in OGICEw
9       |  $\mathbf{a} \leftarrow (\mathbf{w}^H \hat{\mathbf{C}}_{\mathbf{x}} \mathbf{w})^{-1} \hat{\mathbf{C}}_{\mathbf{x}} \mathbf{w}$ ;
10      else
11       | Update  $\mathbf{a}$  as in OGICEa
12       |  $\mathbf{w} \leftarrow (\mathbf{a}^H \hat{\mathbf{C}}_{\mathbf{x}}^{-1} \mathbf{a})^{-1} \hat{\mathbf{C}}_{\mathbf{x}}^{-1} \mathbf{a}$ ;
13      end
14 until  $\|\Delta\| < \text{tol}$ ;

```

The double-striking font will be used to denote concatenated variables or parameters from K mixtures, e.g., $\mathbf{x} = [\mathbf{x}^1; \dots; \mathbf{x}^K]$. The joint mixing matrix obeys $\mathbf{A}_{\text{IVE}} = \text{bdiag}(\mathbf{A}_{\text{ICE}}^1, \dots, \mathbf{A}_{\text{ICE}}^K)$, where $\text{bdiag}(\cdot)$ denotes a block-diagonal matrix with the arguments on the main block-diagonal.

Although the mixtures $\mathbf{x}^1, \dots, \mathbf{x}^K$ are algebraically independent, similarly to IVA, we introduce a joint statistical model (similarly to (12)) given by

$$p_{\mathbf{v}}(\mathbf{v}) = p_{\mathbf{s}}(\mathbf{s})p_{\mathbf{z}}(\mathbf{z}), \quad (52)$$

which means that \mathbf{s} and \mathbf{z} are independent but the elements inside of them can be dependent. Like in the previous section, we constrain our considerations to the Gaussian background modeling; so it is assumed that

$$\mathbf{z} \sim \mathcal{CN}(\mathbf{0}, \mathbf{C}_{\mathbf{z}}), \quad (53)$$

where $\mathbf{C}_{\mathbf{z}} = \text{E}[\mathbf{z}\mathbf{z}^H]$ whose ij th block of dimension $(d-1) \times (d-1)$ is $\mathbf{C}_{\mathbf{z}}^{ij} = \text{E}[\mathbf{z}^i \mathbf{z}^j{}^H]$; similarly $\mathbf{C}_{\mathbf{x}}$ as well as the sample-based counterparts $\hat{\mathbf{C}}_{\mathbf{z}}$ and $\hat{\mathbf{C}}_{\mathbf{x}}$ are defined.

Similar to (26), the quasi-likelihood contrast function following from (52) (for one signal sample), is

$$\mathcal{J}(\mathbf{w}, \mathbf{a}) = \log f(\hat{\mathbf{s}}^1, \dots, \hat{\mathbf{s}}^K) - \sum_{i=1}^K \sum_{j=1}^K \mathbf{x}^{iH} \mathbf{B}^j \mathbf{R}^{ij} \mathbf{B}^j \mathbf{x}^j + \sum_{k=1}^K \log |\det \mathbf{W}_{\text{ICE}}^k|^2, \quad (54)$$

where $\hat{\mathbf{s}}^k = (\mathbf{w}^k)^H \mathbf{x}^k$, and \mathbf{R}^{ij} is a weighting matrix substituting the ij th block of the unknown $\mathbf{C}_{\mathbf{z}}^{-1}$.

B. Gradient of the contrast function

After a lengthy computation, which follows steps similar to those described in Appendix C (we skip the details to save space), the derivative of \mathcal{J} with respect to $(\mathbf{w}^k)^H$ under the constraints (similar to (23))

$$\mathbf{a}^k = \frac{\widehat{\mathbf{C}}_{\mathbf{x}}^{kk} \mathbf{w}^k}{\mathbf{w}^{kH} \widehat{\mathbf{C}}_{\mathbf{x}}^{kk} \mathbf{w}^k}, \quad k = 1, \dots, K, \quad (55)$$

and when $\mathbf{R}^{k\ell}$ is selected as the $k\ell$ th block of $\widehat{\mathbf{C}}_{\mathbf{z}}^{-1}$, reads

$$\frac{\partial \mathcal{J}}{\partial \mathbf{w}^{kH}} = \mathbf{a}^k - \frac{1}{N} \mathbf{X}^k \phi^k(\widehat{\mathbf{s}}^1, \dots, \widehat{\mathbf{s}}^K)^T + \frac{1}{\mathbf{w}^{kH} \widehat{\mathbf{C}}_{\mathbf{x}}^{kk} \mathbf{w}^k} \widehat{\mathbf{C}}_{\mathbf{x}}^{kk} \mathbf{B}^{kH} \boldsymbol{\epsilon}^k. \quad (56)$$

Here, $\widehat{\mathbf{s}}^k = (\mathbf{w}^k)^H \mathbf{X}^k$,

$$\phi^k(\xi^1, \dots, \xi^K) = -\frac{\partial \log f(\xi^1, \dots, \xi^K)}{\partial \xi^k}, \quad (57)$$

is the score function related to the model joint density $f(\cdot)$ of \mathbf{s} with respect to the k th variable, and

$$\boldsymbol{\epsilon}^k = \sum_{\ell=1}^K \mathbf{R}^{k\ell} \boldsymbol{\theta}^{\ell k}, \quad \text{where } \boldsymbol{\theta}^{\ell k} = \widehat{\mathbf{Z}}^{\ell} (\widehat{\mathbf{s}}^k)^H / N. \quad (58)$$

By comparing (33) with (56), the latter differs only in that the nonlinearity $\phi^k(\cdot)$ is dependent on the SOIs separated from all K mixtures, plus the third term that does not occur in (33).

$\boldsymbol{\theta}^{\ell k}$ is the sample correlation between the estimated SOI in the k th mixture and the separated background in the ℓ th mixture, and can also be written as $\boldsymbol{\theta}^{\ell k} = \mathbf{B}^{\ell} \widehat{\mathbf{C}}_{\mathbf{x}}^{\ell k} \mathbf{w}^k$. For $k = 1, \dots, K$, $\boldsymbol{\theta}^{kk} = \mathbf{0}$ due to the OG, but, for $k \neq \ell$, $\boldsymbol{\theta}^{\ell k}$ is non-zero in general. Therefore, the third term in (56) vanishes only when $\mathbf{R}^{k\ell} = \mathbf{0}$ for $k \neq \ell$, $\ell = 1, \dots, K$.

Here, a special case is worth considering in which $\mathbf{C}_{\mathbf{x}} = \text{bdiag}(\mathbf{C}_{\mathbf{x}}^{11}, \dots, \mathbf{C}_{\mathbf{x}}^{KK})$; in other words, the mixtures (50) are uncorrelated (each from the other), and there are only higher-order dependencies, if any. Then, $\mathbf{C}_{\mathbf{z}}$ has the same block-diagonal structure as $\mathbf{C}_{\mathbf{x}}$, so it is reasonable to select $\mathbf{R}^{k\ell} = \mathbf{0}$ for $k \neq \ell$, although the sample covariances $\widehat{\mathbf{C}}_{\mathbf{z}}^{k\ell}$ are not exactly zero. In that case, (56) is simplified to (compare with (33))

$$\frac{\partial \mathcal{J}}{\partial \mathbf{w}^{kH}} = \mathbf{a}^k - \frac{1}{N} \mathbf{X}^k \phi^k(\widehat{\mathbf{s}}^1, \dots, \widehat{\mathbf{s}}^K)^T. \quad (59)$$

This observation is in agreement with the literature. The joint separation of correlated mixtures can be achieved using only second-order statistics [6], [51]. Uncorrelated mixtures arise, for instance, in the frequency-domain separation of convolutive mixtures. Here, the non-Gaussianity and higher-order moments are necessary for separating the mixtures [9], [52].

C. Gradient algorithms for IVE

The constrained gradient can, similarly to (59) and (37), be computed with respect to $(\mathbf{a}^k)^H$, which gives (we skip the detailed computation)

$$\frac{\partial \mathcal{J}}{\partial \mathbf{a}^{kH}} = \mathbf{w}^k - \frac{\lambda_{\mathbf{a}}^k}{N} (\widehat{\mathbf{C}}_{\mathbf{x}}^{kk})^{-1} \mathbf{X}^k \phi^k(\widehat{\mathbf{s}}^1, \dots, \widehat{\mathbf{s}}^K)^T, \quad (60)$$

where $\lambda_{\mathbf{a}}^k = (\mathbf{a}^{kH} (\widehat{\mathbf{C}}_{\mathbf{x}}^{kk})^{-1} \mathbf{a}^k)^{-1}$. Now, the gradient optimization algorithms for IVE (considering only sets of uncorrelated instantaneous mixtures) can proceed in the same way as those for ICE with the following differences:

- 1) In each iteration, \mathbf{w}_k or \mathbf{a}_k are updated by adding a step in the direction of the gradient (59) or (60), respectively, for each $k = 1, \dots, K$.
- 2) The nonlinear functions ϕ^k , $k = 1, \dots, K$, depend on the current outputs of all K iterative algorithms, which fact makes them mutually dependent.

We will refer to these algorithms as to $\text{OGIVE}_{\mathbf{w}}$ and $\text{OGIVE}_{\mathbf{a}}$, respectively; for illustration, $\text{OGIVE}_{\mathbf{w}}$ is described in Algorithm 3.

Algorithm 3: $\text{OGIVE}_{\mathbf{w}}$: orthogonally constrained extraction of an independent vector component from the set of mutually uncorrelated mixtures $\mathbf{X}^1, \dots, \mathbf{X}^K$

Input: $\mathbf{X}^k, \mathbf{w}_{\text{ini}}^k$, $k = 1, \dots, K$, μ , tol

Output: $\mathbf{a}^k, \mathbf{w}^k$, $k = 1, \dots, K$

```

1 foreach  $k = 1, \dots, K$  do
2    $\hat{\mathbf{C}}_{\mathbf{x}}^{kk} = \mathbf{X}^k (\mathbf{X}^k)^H / N$ ;
3    $\mathbf{w}^k = \mathbf{w}_{\text{ini}}^k$ ;
4 end
5 repeat
6   foreach  $k = 1, \dots, K$  do
7      $\mathbf{a}^k \leftarrow ((\mathbf{w}^k)^H \hat{\mathbf{C}}_{\mathbf{x}}^{kk} \mathbf{w}^k)^{-1} \hat{\mathbf{C}}_{\mathbf{x}}^{kk} \mathbf{w}^k$ ;
8      $\hat{\mathbf{s}}^k \leftarrow (\mathbf{w}^k)^H \mathbf{X}^k$ ;
9   end
10  foreach  $k = 1, \dots, K$  do
11     $\nu^k \leftarrow \hat{\mathbf{s}}^k \phi^k(\hat{\mathbf{s}}^1, \dots, \hat{\mathbf{s}}^K)^T / N$ ;
12     $\Delta^k \leftarrow \mathbf{a}^k - (\nu^k)^{-1} \mathbf{X}^k \phi^k(\hat{\mathbf{s}}^1, \dots, \hat{\mathbf{s}}^K)^T / N$ ;
13     $\mathbf{w}^k \leftarrow \mathbf{w}^k + \mu \Delta^k$ ;
14  end
15 until  $\max\{\|\Delta^1\|, \dots, \|\Delta^K\|\} < \text{tol}$ ;

```

Finally, we introduce a method referred to as $\text{OGIVE}_{\mathbf{s}}$, where the idea presented in Section III-F is applied within each mixture. The parameter in which the gradient optimization proceeds is selected based on the heuristic criterion (49). It is important that the selection can be different for each mixture.

In fact, this approach inherently assumes that the behavior of the optimization process within any mixture is similar as in case of ICE. The behavior can be different in case of IVE as the parallel extraction algorithms influence each other. The advantage of this feature is that the dependence can bring a synergic effect: When most initial separating/mixing vectors lie in the ROC of the SOI, the convergence within the other mixtures can be enforced.

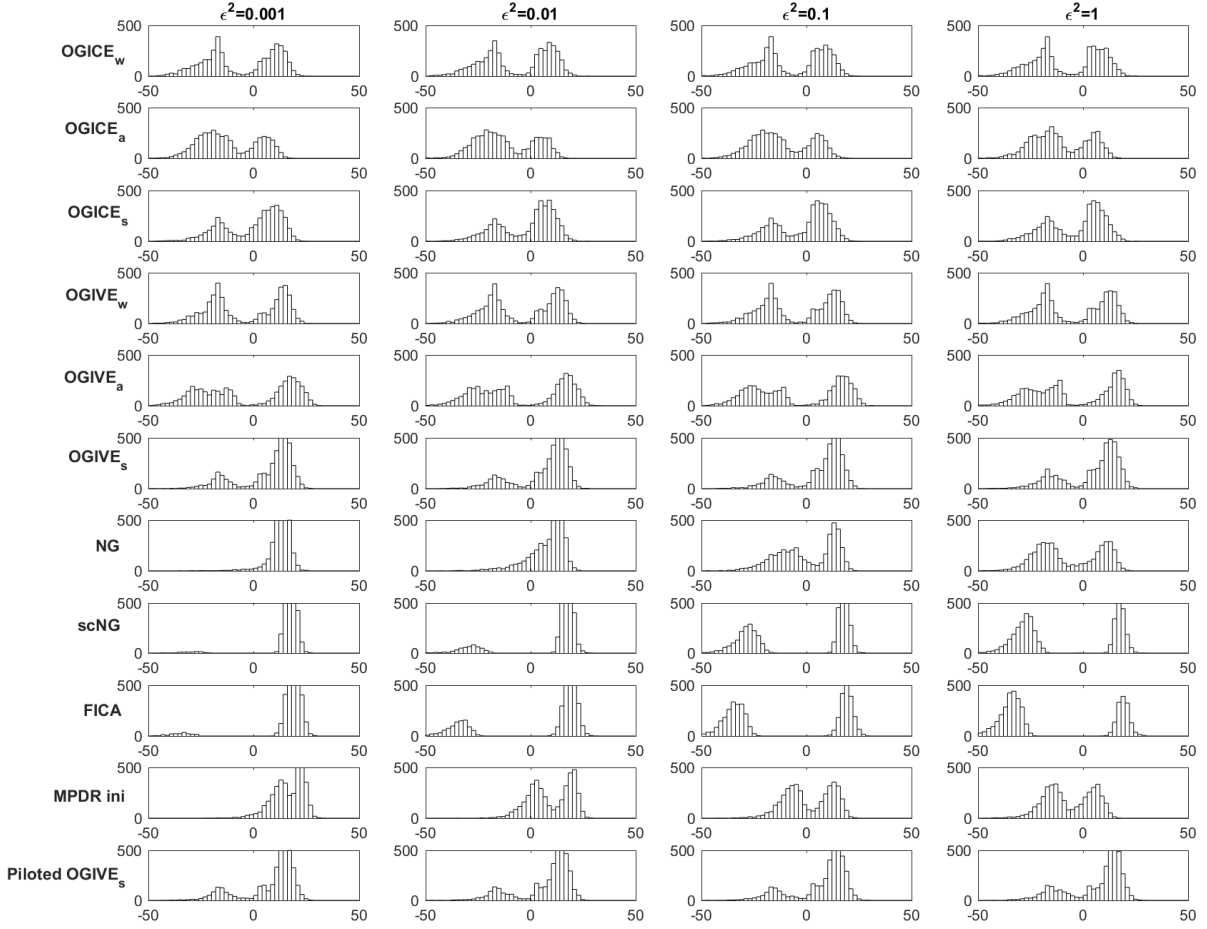


Fig. 2. Histograms of the output SIR (in dB) achieved by the blind algorithms in 1000 trials (4000 extractions) when the background is Laplacean.

V. SIMULATIONS

In simulations, we focus on the sensitivity of the proposed ICE and IVE algorithms to the initialization and compare them with other methods. In one simulated trial, K instantaneous mixtures are generated with random mixing matrices \mathbf{A}^k , $k = 1, \dots, K$. The SOIs for these mixtures are obtained as K signals drawn independently from the Laplacean distribution and mixed by a random unitary matrix; hence, they are uncorrelated and dependent. The background is obtained by generating independent components u_2^k, \dots, u_d^k from the Gaussian or Laplacean distribution, $k = 1, \dots, K$; all the distributions are circular.

For each mixture, the SR is selected randomly either -10 or 10 dB. The mixing matrices are drawn from the uniform distribution; the real part in $[1; 2]$ and the imaginary part in $[0, 1]$. This choice helps us keep the initial SIR approximately equal across all input channels, that is, less dependent on the mixing matrix while mostly dependent of the SR.

The comparison involves One-Unit FastICA (FICA) [53], three variants of OGICE proposed in Section III, the Natural Gradient algorithm (NG) [49] and its scaled version (scNG) [54], which is frequently used in audio separation methods, as well as three variants of OGIVE proposed in Section IV-C. These algorithms are

TABLE I
DETAILED SETTINGS OF THE COMPARED METHODS

Algorithm(s)	maximum # iterations	stopping threshold	step length
OGICE variants	5×10^3	10^{-3}	0.1
OGIVE variants	4×10^3	10^{-3}	0.1
NG, scNG	5×10^3	10^{-3}	0.02
FICA	1×10^3	10^{-6}	-

initialized by $\mathbf{a}_{\text{ini}} = \mathbf{a} + \mathbf{e}_{\text{ini}}$, where \mathbf{a} is the true mixing vector, and \mathbf{e}_{ini} is a random vector which is orthogonal to \mathbf{a} , and $\|\mathbf{e}_{\text{ini}}\|^2 = \epsilon^2$. The algorithms NG and scNG are initialized by the de-mixing matrix whose first row is equal to (22) where $\mathbf{a} = \mathbf{a}_{\text{ini}}$; the other rows are selected as in (8), which means that the initial background subspace is orthogonal to the initial SOI estimate.

Next, we also evaluate the SOI estimates obtained through (22) for \mathbf{a} equal to the true mixing vector (MPDR_oracle) and for $\mathbf{a} = \mathbf{a}_{\text{ini}}$ (MPDR_ini). While the performance of the MPDR_oracle gives an upper bound, that of MPDR_ini corresponds to a “do-nothing” solution purely relying on the initialization.

ICE/ICA methods are applied to each mixture separately, while IVE algorithms treat all K mixtures jointly³. The nonlinearity $\phi(\xi) = \overline{\tanh}(\xi)$ is selected in the variants of OGICE and NG. FICA is used with $(1 + |\xi|^2)^{-1}$. For IVE algorithms, the choice is

$$\phi^k(\xi^1, \dots, \xi^K) = \overline{\tanh}(\xi^k) / \sqrt{\sum_{\ell=1}^K |\xi^\ell|^2}. \quad (61)$$

The problem of choosing an appropriate nonlinearity for the given method would go beyond the scope of this paper; see, e.g., [28], [45].

For the sake of completeness, we also include a semi-blind variant of OGIVE_s, which is modified in a way similar to that proposed in [55]. Specifically, a “pilot” component p is assumed to be available such that the SOIs within the K mixtures are dependent on it (usually there are only higher-order dependencies; see [9]). OGIVE_s is modified only by adding the $K + 1$ th variable into (61), which is $\xi_{K+1} = p$. In simulations, p is a random mixture of the SOIs. This method will be referred to as “Piloted OGIVE_s”.

The detailed settings of the compared algorithms are shown in Table I; these values were selected to ensure good performance of the methods.

A. Results

The algorithms were tested in 1000 independent trials for $d = 6$, $K = 4$, and $N = 1000$. Each extracted signal was assessed by the output SIR (the ratio of powers of the SOI and of the other signals within the extracted signal). In the experiment, the achieved SIRs range from -50 through 50 dB depending on whether

³IVE can take advantage of the dependence among SOIs from different mixtures while ICA/ICE cannot. The intention here is not to favor IVE prior to ICE; the goal is to evaluate the contribution due to the joint extraction.

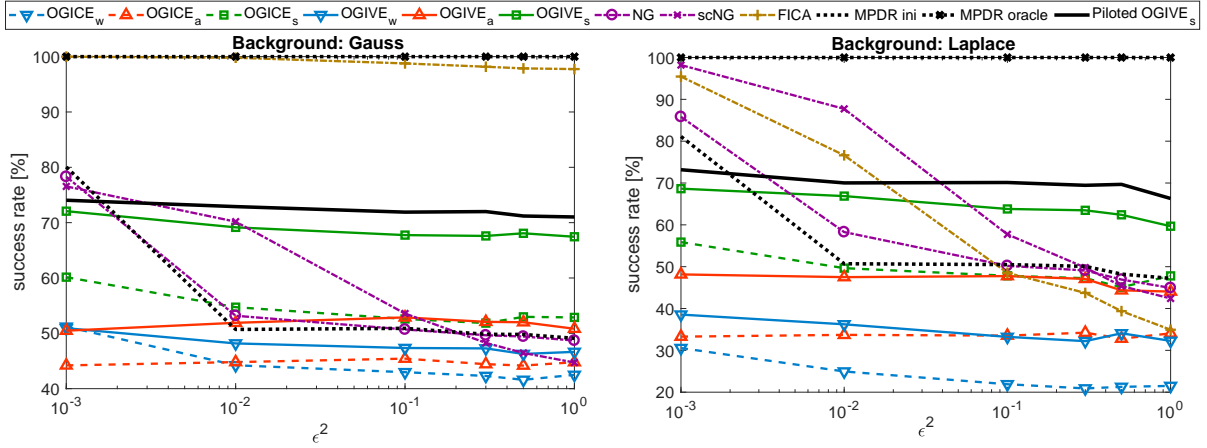


Fig. 3. Success rates as functions of the initial mean squared error ϵ^2 for $d = 6$, $K = 4$, and $N = 1000$. The experiment was repeated in 1000 trials ($1000 \times K$ mixtures). The SOI is generated from Laplace components while the background is Gaussian or Laplacean.

the SOI was extracted or a different source, and the SIR also depends on the qualities of the given algorithm. Complete results achieved by the methods, for the Laplacean background, are shown in Fig. 2 as histograms.

Since our primary focus is on the extraction of the SOI, the results in Fig. 3 show the percentages of successful extractions of the SOI (success rates) as functions of the initial error $\|\mathbf{e}_{\text{ini}}\|^2 = \epsilon^2$. Here, each extraction is classed as *successful* if the output SIR is greater than 0 dB. We first discuss these results as follows.

- 1) **MPDR:** MPDR oracle achieves 100% success rate. The success rate of MPDR_ini is decaying with growing ϵ^2 as MPDR_ini yields SIR corresponding to the extracted signal using the initial mixing vector. Its success rate approaches 50% as $\epsilon^2 \rightarrow 1$, which corresponds with the fact that $\text{SR} = 10$ dB in about 50% of trials. The results of MPDR_oracle and of MPDR_ini do not depend on the signals' distributions.
- 2) **OGICE_{a/w}:** OGICE_a and OGICE_w achieve success rate 20-50% almost independently of ϵ^2 . This corresponds with the fact that maximum 50% of trials are advantageous for each method ($\text{SR} = -10$ dB for OGICE_a and $\text{SR} = +10$ dB for OGICE_w). The success rates are mostly lower than 50%, which shows that also the mixing matrix has an influence of the ROC of the SOI, so, for example, $\text{SR} = +10$ dB does not always guarantee that OGICE_w converges to the SOI from almost any initial value⁴. For the Laplacean background, the success rates are lower than for the Gaussian background because there is a higher probability that the methods are attracted by a different non-Gaussian source.
- 3) **OGIVE_{a/w}:** The IVE counterparts of OGICE_a and OGICE_w perform similarly but their success rates are always closer to 50%. This is caused by the joint extraction. OGIVE_a and OGIVE_w take advantage of the dependence between the SOIs in K mixtures, which improves the overall convergence.
- 4) **Switched optimization:** In terms of the success rate, OGICE_s and OGIVE_s achieve significant improvements compared to OGICE_{a/w} and OGIVE_{a/w}, respectively. This points to the effectiveness of the decision rule based on the criterion (49) and to the synergy of the joint separation in case of OGIVE_s. It is worth

⁴It can be verified, by repeating this experiment, that with $\text{SR} = \pm 15$ dB, OGICE_{a/w} achieve almost 50% success rate. It means that with a higher range of SR the influence of the mixing matrix (generated in the same vein as in this experiment) is lower.

pointing to the fact that the performance of OGICE_s and OGIVE_s is slightly decreasing with growing ϵ^2 . This is because for higher ϵ^2 , the initial mixing vector is more distant from the true value, so the criterion (49) is less reliable for the selection of the optimization parameter. To avoid this drawback, a better decision rule or partial knowledge of SR) is needed.

- 5) **NG and scNG:** The success rate of these ICA algorithms significantly depends on the initial error and also on the distribution of the background. The success rate is superior for very small values of ϵ^2 , but it rapidly drops with growing ϵ^2 (scNG appears to be less sensitive than NG). The results also show that very good convergence is achieved for $\epsilon^2 < 10^{-2}$ when the background is Laplacean. This points to the fact that ICA algorithms can take advantage of the non-Gaussianity of background signals.
- 6) **FICA** shows excellent results when the background is Gaussian. Since it is a fixed-point algorithm, it has good ability to avoid shallow extremes of the contrast function that correspond to Gaussian components. Therefore, its global convergence is very good when there are no other non-Gaussian components than the SOI. For the same reason, the success rate of FICA is dropping down with growing ϵ^2 when the background is Laplacean.
- 7) **Piloted OGIVE_s :** This algorithm gives a higher success rate than OGIVE_s as it exploits the pilot dependent component to keep converging to the SOI. Its performance is slightly decreasing when ϵ^2 grows due to the shortage of the criterion (49), as mentioned in Item 4 above.

Now we go back to the histograms of the output SIR (in dB) shown in Fig. 2. Typically, the values are concentrated around two peaks with central value $\approx \pm 20$ dB. When more values are concentrated around the positive SIR for any ϵ^2 , the given method shows good robustness against the initialization error as it mostly tends to keep converging to the SOI. From this perspective, OGICE_s , OGIVE_s and Piloted OGIVE_s show the best results, which was already discussed above.

The variance of the SIRs around the peaks reflect the ability of the method to avoid local extremes of the contrast function and/or its ability to converge before the maximum number of iterations is reached. In this respect, scNG and FICA achieve superior results as they rarely yield an output SIRs within the range $[-10, 10]$ dB. It is worth pointing out that scNG and FICA could be interpreted as gradient methods using adaptive step lengths, as discussed in Section III-E for the case of FICA. The other compared algorithms, the variants of OGICE and of OGIVE and NG, utilize constant step lengths. Their histograms are less concentrated around the main peaks, which means that they often stack in a local extreme or converge too slowly to achieve the desired extreme of the contrast function.

VI. CONCLUSIONS

We have revised the problem of blind source extraction of an independent target source from background signals. The maximum likelihood approach where the mixing model is parameterized for the extraction of one source and where the background signals are modeled as a Gaussian mixture was introduced as Independent Component Extraction (ICE). Similarly, Independent Vector Extraction (IVE) was introduced for the joint extraction problem.

Several variants of gradient algorithms have been derived. Our attention has been focused on their region of convergence (ROC) related to the source of interest (SOI). It was shown that the size of the ROC is not only algorithm-dependent but it also strongly depends on the ratio of scales of the sources within the mixture. In particular, we have shown that the size of the ROC can be influenced through the selection of optimization parameters. This was corroborated by simulations where the methods endowed with the automatic selection of optimization parameters achieved a high rate of successful extractions of the SOI, almost independent of the initialization.

The simulation study also confirmed that the joint extraction through IVE brings advantageous features compared ICE. In particular, the IVE methods with the automatic selection show synergistic convergence, by which we mean that simultaneous converge to the SOIs within several mixtures help to enforce the convergence also in the other mixtures.

Next, the gradient algorithms derived based on ICE have been compared with the Natural Gradient-based methods for ICA and with One-Unit FastICA. Close connections between the methods have been revealed, which sheds light on the relation between ICE and the well known blind source separation/extraction (BSS/BSE) methods. In particular, the importance of the orthogonal constraint (the orthogonality of the subspaces spanned by the SOI and the background signals) and the Gaussian modeling of the background signals in ICE methods was shown. Therefore, future works should be focused on these aspects in order to improve overall properties of ICE/IVE algorithms in non-Gaussian background and also in underdetermined scenarios.

APPENDIX A: PROOF OF (22) AND (23)

Since $\mathbf{y} = \mathbf{Qz} = \mathbf{QBx}$, we can introduce the projection operator $\mathbf{\Pi}_y = \mathbf{QB}$, which is equal to

$$\mathbf{\Pi}_y = \mathbf{I}_d - \mathbf{aw}^H. \quad (62)$$

According to (21), the OC can be written as

$$\widehat{\mathbf{Z}}^H \widehat{\mathbf{s}}/N = \mathbf{B}\widehat{\mathbf{C}}_x \mathbf{w} = \mathbf{0}. \quad (63)$$

By multiplying the latter equation from the left by \mathbf{Q} and using (62), we arrive at

$$(\mathbf{I}_d - \mathbf{aw}^H)\widehat{\mathbf{C}}_x \mathbf{w} = \mathbf{0}, \quad (64)$$

$$\mathbf{w} - \widehat{\mathbf{C}}_x^{-1} \mathbf{a} (\mathbf{w}^H \widehat{\mathbf{C}}_x \mathbf{w}) = \mathbf{0}. \quad (65)$$

By multiplying (65) from the left by \mathbf{a}^H it follows

$$\mathbf{a}^H \mathbf{w} - \mathbf{a}^H \widehat{\mathbf{C}}_x^{-1} \mathbf{a} \mathbf{w}^H \widehat{\mathbf{C}}_x \mathbf{w} = 0, \quad (66)$$

and since $\mathbf{a}^H \mathbf{w} = 1$, it holds that

$$\mathbf{a}^H \widehat{\mathbf{C}}_x^{-1} \mathbf{a} = (\mathbf{w}^H \widehat{\mathbf{C}}_x \mathbf{w})^{-1}. \quad (67)$$

By putting (65) and (67) together, (22) and (23) follow. ■

APPENDIX B: PROOF OF (25)

Assume that \mathbf{a} is equal to its true value in (2) (hence $\mathbf{A} = \mathbf{A}_{\text{ICE}}$ and $\mathbf{W} = \mathbf{W}_{\text{ICE}}$), and recall that, in the determined ICE model, $\mathbf{y} = \mathbf{Qz}$ holds. Then, $\mathbf{w}_{\text{MPDR}}^H \mathbf{x} = s + \mathbf{w}_{\text{MPDR}}^H \mathbf{y}$. We should show that $\mathbf{a}^H \mathbf{C}_x^{-1} \mathbf{y} = \mathbf{0}$. It holds that

$$\mathbf{a}^H \mathbf{C}_x^{-1} \mathbf{y} = \mathbf{a}^H \mathbf{C}_x^{-1} \mathbf{Qz} \quad (68)$$

$$= \mathbf{a}^H (\mathbf{A} \mathbf{C}_v \mathbf{A}^H)^{-1} \mathbf{Qz} \quad (69)$$

$$= \mathbf{a}^H \mathbf{W}^H \mathbf{C}_v^{-1} \mathbf{W} \mathbf{Qz}, \quad (70)$$

where $\mathbf{C}_v = \mathbb{E}[\mathbf{v}\mathbf{v}^H]$. Next, it holds that $\mathbf{a}^H \mathbf{W}^H = [1, \mathbf{0}^H]$, and $\mathbf{W} \mathbf{Q} = [\mathbf{0}, \mathbf{I}_{d-1}]^H$. By taking into account the block-diagonal structure of \mathbf{C}_v , i.e.,

$$\mathbf{C}_v = \begin{pmatrix} \sigma_s^2 & \mathbf{0}^H \\ \mathbf{0} & \mathbf{C}_z \end{pmatrix}, \quad (71)$$

where σ_s^2 denotes the variance of s , (25) follows. \blacksquare

APPENDIX C: COMPUTATION OF (27)

The following identities hold under the constraint (23).

$$\mathbf{g} = \mathbf{E} \mathbf{a} = \frac{\mathbf{E} \widehat{\mathbf{C}}_x \mathbf{w}}{\mathbf{w}^H \widehat{\mathbf{C}}_x \mathbf{w}}, \quad (72)$$

$$\gamma = \mathbf{e}_1^H \mathbf{a} = \frac{\mathbf{e}_1^H \widehat{\mathbf{C}}_x \mathbf{w}}{\mathbf{w}^H \widehat{\mathbf{C}}_x \mathbf{w}}, \quad (73)$$

$$1 - \mathbf{h}^H \mathbf{g} = \bar{\beta} \gamma = \bar{\beta} \frac{\mathbf{e}_1^H \widehat{\mathbf{C}}_x \mathbf{w}}{\mathbf{w}^H \widehat{\mathbf{C}}_x \mathbf{w}}. \quad (74)$$

To derive (27), we proceed by computing the derivatives of the three terms in (26). First, using (28), it follows that

$$\frac{\partial}{\partial \mathbf{w}^H} \log f(\mathbf{w}^H \mathbf{x}) = -\phi(\mathbf{w}^H \mathbf{x}) \mathbf{x}, \quad (75)$$

so that

$$\frac{1}{N} \sum_{n=1}^N -\phi(\mathbf{w}^H \mathbf{x}(n)) \mathbf{x}(n) = -\frac{1}{N} \mathbf{X} \phi(\mathbf{w}^H \mathbf{X})^T, \quad (76)$$

where $\phi(\cdot)$ is applied element-wise in case of the vector argument.

Let \mathbf{x} be partitioned as $\mathbf{x} = [x_1; \mathbf{x}_2]$. Under the constraint (23) and using $\mathbf{B} = [\mathbf{g}, -\gamma \mathbf{I}_{d-1}]$, the second term in (26) (where the argument n is omitted) can be re-written as

$$\begin{aligned} \mathbf{x}^H \mathbf{B}^H \mathbf{R} \mathbf{B} \mathbf{x} &= (\mathbf{w}^H \widehat{\mathbf{C}}_x \mathbf{w})^{-1} \times \\ & \left(|x_1|^2 \mathbf{w}^H \widehat{\mathbf{C}}_x \mathbf{E}^H \mathbf{R} \mathbf{E} \widehat{\mathbf{C}}_x \mathbf{w} - \bar{x}_1 \mathbf{w}^H \widehat{\mathbf{C}}_x \mathbf{E}^H \mathbf{e}_1 \widehat{\mathbf{C}}_x \mathbf{w} \mathbf{R} \mathbf{x}_2 - \right. \\ & \left. x_1 \mathbf{w}^H \widehat{\mathbf{C}}_x \mathbf{e}_1 \mathbf{x}_2^H \mathbf{R} \mathbf{E} \widehat{\mathbf{C}}_x \mathbf{w} + \mathbf{w}^H \widehat{\mathbf{C}}_x \mathbf{e}_1 \mathbf{x}_2^H \mathbf{R} \mathbf{e}_1 \widehat{\mathbf{C}}_x \mathbf{w} \mathbf{x}_2 \right). \quad (77) \end{aligned}$$

By taking the derivative under the OG and after some rearrangements,

$$\begin{aligned} \frac{\partial}{\partial \mathbf{w}^H} \mathbf{x}^H \mathbf{B}^H \mathbf{R} \mathbf{B} \mathbf{x} &= -2\mathbf{a} \mathbf{x}^H \mathbf{B}^H \mathbf{R} \mathbf{B} \mathbf{x} + \\ & (\mathbf{w}^H \widehat{\mathbf{C}}_x \mathbf{w})^{-1} \times (\bar{x}_1 \widehat{\mathbf{C}}_x \mathbf{E}^H \mathbf{R} \mathbf{B} \mathbf{x} - \mathbf{x}_2^H \mathbf{R} \mathbf{B} \mathbf{x} \widehat{\mathbf{C}}_x \mathbf{e}_1). \quad (78) \end{aligned}$$

By considering the averages of the above terms over N samples, we arrive at the following chain of identities:

$$\begin{aligned} \frac{1}{N} \sum_{n=1}^N \mathbf{x}(n)^H \mathbf{B}^H \mathbf{R} \mathbf{B} \mathbf{x}(n) &= \frac{1}{N} \sum_{n=1}^N \text{tr}(\mathbf{B}^H \mathbf{R} \mathbf{B} \mathbf{x}(n) \mathbf{x}(n)^H) \\ &= \text{tr}(\mathbf{R} \widehat{\mathbf{C}}_{\mathbf{x}} \mathbf{B}^H) = \text{tr}(\mathbf{R} \widehat{\mathbf{C}}_{\mathbf{z}}). \end{aligned} \quad (79)$$

Next,

$$\begin{aligned} \frac{1}{N} \sum_{n=1}^N \bar{x}_1(n) \widehat{\mathbf{C}}_{\mathbf{x}} \mathbf{E}^H \mathbf{R} \mathbf{B} \mathbf{x}(n) &= \widehat{\mathbf{C}}_{\mathbf{x}} \mathbf{E}^H \mathbf{R} \mathbf{B} \mathbf{X} \mathbf{X}^H \mathbf{e}_1 / N \\ &= \widehat{\mathbf{C}}_{\mathbf{x}} \mathbf{E}^H \mathbf{R} \widehat{\mathbf{Z}} \mathbf{X}^H \mathbf{e}_1 / N \\ &= \widehat{\mathbf{C}}_{\mathbf{x}} \mathbf{E}^H \mathbf{R} \widehat{\mathbf{Z}} \begin{pmatrix} \widehat{\mathbf{s}}^H & \widehat{\mathbf{z}}^H \end{pmatrix} \mathbf{A}_{\text{ICE}}^H \mathbf{e}_1 / N \\ &= \widehat{\mathbf{C}}_{\mathbf{x}} \mathbf{E}^H \mathbf{R} \begin{pmatrix} \mathbf{0}^H & \widehat{\mathbf{C}}_{\mathbf{z}} \end{pmatrix} \mathbf{A}_{\text{ICE}}^H \mathbf{e}_1 \\ &= \widehat{\mathbf{C}}_{\mathbf{x}} \mathbf{E}^H \mathbf{R} \widehat{\mathbf{C}}_{\mathbf{z}} \mathbf{h}, \end{aligned} \quad (80)$$

where we used (20) and (21). The last identity is

$$\frac{1}{N} \sum_{n=1}^N \mathbf{x}_2^H \mathbf{R} \mathbf{B} \mathbf{x} \widehat{\mathbf{C}}_{\mathbf{x}} \mathbf{e}_1 = \text{tr}(\mathbf{R} \widehat{\mathbf{C}}_{\mathbf{x}} \mathbf{E}^H) \widehat{\mathbf{C}}_{\mathbf{x}} \mathbf{e}_1. \quad (81)$$

The derivative of the third term in (26) reads

$$\begin{aligned} (d-2) \frac{\partial}{\partial \mathbf{w}^H} \log |\gamma|^2 &= \\ (d-2) \frac{\partial}{\partial \mathbf{w}^H} (\log |\mathbf{w}^H \widehat{\mathbf{C}}_{\mathbf{x}} \mathbf{e}_1|^2 - \log |\mathbf{w}^H \widehat{\mathbf{C}}_{\mathbf{x}} \mathbf{w}|^2) &= \\ (d-2) \frac{\partial}{\partial \mathbf{w}^H} (\log \mathbf{w}^H \widehat{\mathbf{C}}_{\mathbf{x}} \mathbf{e}_1 - 2 \log \mathbf{w}^H \widehat{\mathbf{C}}_{\mathbf{x}} \mathbf{w}) &= \\ (d-2) \left(\frac{\widehat{\mathbf{C}}_{\mathbf{x}} \mathbf{e}_1}{\mathbf{w}^H \widehat{\mathbf{C}}_{\mathbf{x}} \mathbf{e}_1} - 2 \frac{\widehat{\mathbf{C}}_{\mathbf{x}} \mathbf{w}}{\mathbf{w}^H \widehat{\mathbf{C}}_{\mathbf{x}} \mathbf{w}} \right) &= \\ (d-2) \left(\gamma^{-1} \frac{\widehat{\mathbf{C}}_{\mathbf{x}} \mathbf{e}_1}{\mathbf{w}^H \widehat{\mathbf{C}}_{\mathbf{x}} \mathbf{w}} - 2 \mathbf{a} \right). \end{aligned} \quad (82)$$

Now, (27) is obtained by putting together (76), (78), and (82) using the identities (79), (80), and (81). ■

REFERENCES

- [1] T.-W. Lee, *Independent Component Analysis - Theory and Applications*. Kluwer Academic Publishers, 1998.
- [2] A. Hyvärinen, J. Karhunen, and E. Oja, *Independent Component Analysis*. John Wiley & Sons, 2001.
- [3] A. Cichocki and S. Amari, *Adaptive Blind Signal and Image Processing*. John Wiley & Sons, 2002.
- [4] P. Comon and C. Jutten, *Handbook of Blind Source Separation: Independent Component Analysis and Applications*, ser. Independent Component Analysis and Applications Series. Elsevier Science, 2010.
- [5] P. Smaragdakis, "Blind separation of convolved mixtures in the frequency domain," *Neurocomputing*, vol. 22, pp. 21–34, 1998.
- [6] Y. O. Li, T. Adali, W. Wang, and V. D. Calhoun, "Joint blind source separation by multiset canonical correlation analysis," *IEEE Transactions on Signal Processing*, vol. 57, no. 10, pp. 3918–3929, Oct 2009.
- [7] D. Lahat and C. Jutten, "Joint blind source separation of multidimensional components: Model and algorithm," in *2014 22nd European Signal Processing Conference (EUSIPCO)*, Sept 2014, pp. 1417–1421.
- [8] X.-L. Li, T. Adali, and M. Anderson, "Joint blind source separation by generalized joint diagonalization of cumulant matrices," *Signal Processing*, vol. 91, no. 10, pp. 2314 – 2322, 2011.

- [9] T. Kim, H. T. Attias, S.-Y. Lee, and T.-W. Lee, "Blind source separation exploiting higher-order frequency dependencies," *IEEE Transactions on Audio, Speech, and Language Processing*, pp. 70–79, Jan. 2007.
- [10] H. Sawada, R. Mukai, S. Araki, and S. Makino, "Solving the permutation and the circularity problem of frequency-domain blind source separation," in *Proc. of the 18th International Congress on Acoustics (ICA 2004)*, Apr. 2004, pp. I-89–I-92.
- [11] Z. Koldovský, J. Málek, P. Tichavský, and F. Nesta, "Semi-blind noise extraction using partially known position of the target source," *IEEE Transactions on Audio, Speech, and Language Processing*, vol. 21, no. 10, pp. 2029–2041, Oct 2013.
- [12] H. Sawada, S. Araki, R. Mukai, and S. Makino, "Blind extraction of a dominant source signal from mixtures of many sources," in *Proceedings of IEEE International Conference on Audio, Speech and Signal Processing*, vol. III, Mar. 2005, pp. 61–64.
- [13] S. Javidi, D. P. Mandic, and A. Cichocki, "Complex blind source extraction from noisy mixtures using second-order statistics," *IEEE Transactions on Circuits and Systems I: Regular Papers*, vol. 57, no. 7, pp. 1404–1416, July 2010.
- [14] S. Amari and A. Cichocki, "Adaptive blind signal processing-neural network approaches," *Proceedings of the IEEE*, vol. 86, no. 10, pp. 2026–2048, Oct 1998.
- [15] S. A. Cruces-Alvarez, A. Cichocki, and S. Amari, "From blind signal extraction to blind instantaneous signal separation: criteria, algorithms, and stability," *IEEE Transactions on Neural Networks*, vol. 15, no. 4, pp. 859–873, July 2004.
- [16] P. J. Huber, "Projection pursuit," *Ann. Statist.*, vol. 13, no. 2, pp. 435–475, June 1985.
- [17] M. Girolami, "Extraction of independent signal sources using a deflationary exploratory projection pursuit network with lateral inhibition," *IEE Proceedings - Vision, Image and Signal Processing*, vol. 144, pp. 299–306(7), October 1997.
- [18] O. Shalvi and E. Weinstein, "Super-exponential methods for blind deconvolution," *IEEE Transactions on Information Theory*, vol. 39, no. 2, pp. 504–519, Mar 1993.
- [19] J. J. Shynk and R. P. Gooch, "The constant modulus array for cochannel signal copy and direction finding," *IEEE Transactions on Signal Processing*, vol. 44, no. 3, pp. 652–660, Mar 1996.
- [20] E. Moreau and O. Macchi, "High-order contrasts for self-adaptive source separation," *International Journal of Adaptive Control and Signal Processing*, vol. 10, no. 1, pp. 19–46, 1996.
- [21] T. Cover and J. Thomas, *Elements of Information Theory*. Wiley, 2006.
- [22] J. F. Cardoso, "Blind signal separation: statistical principles," *Proceedings of the IEEE*, vol. 86, no. 10, pp. 2009–2025, Oct 1998.
- [23] N. Delfosse and P. Loubaton, "Adaptive blind separation of independent sources: A deflation approach," *Signal Processing*, vol. 45, no. 1, pp. 59 – 83, 1995.
- [24] A. T. Erdogan, "On the convergence of ica algorithms with symmetric orthogonalization," *IEEE Transactions on Signal Processing*, vol. 57, no. 6, pp. 2209–2221, June 2009.
- [25] A. Hyvärinen and E. Oja, "A fast fixed-point algorithm for independent component analysis," *Neural Computation*, vol. 9, no. 7, pp. 1483–1492, July 1997.
- [26] A. Hyvärinen, "Fast and robust fixed-point algorithm for independent component analysis," *IEEE Transactions on Neural Networks*, vol. 10, no. 3, pp. 626–634, 1999.
- [27] T. Wei, "A convergence and asymptotic analysis of the generalized symmetric fastica algorithm," *IEEE Transactions on Signal Processing*, vol. 63, no. 24, pp. 6445–6458, Dec 2015.
- [28] P. Tichavský, Z. Koldovský, and E. Oja, "Performance analysis of the FastICA algorithm and Cramér-Rao bounds for linear independent component analysis," *IEEE Transactions on Signal Processing*, vol. 54, no. 4, pp. 1189–1203, April 2006.
- [29] A. Hyvärinen, "One-unit contrast functions for independent component analysis: a statistical analysis," in *Neural Networks for Signal Processing VII. Proceedings of the 1997 IEEE Signal Processing Society Workshop*, Sep 1997, pp. 388–397.
- [30] J.-F. Cardoso, "On the performance of orthogonal source separation algorithms," in *Proceedings of European Signal Processing Conference*, Sep. 1994, pp. 776–779.
- [31] Z. Koldovský, P. Tichavský, and E. Oja, "Efficient variant of algorithm FastICA for independent component analysis attaining the Cramér-Rao lower bound," *IEEE Transactions on Neural Networks*, vol. 17, no. 5, pp. 1265–1277, Sept 2006.
- [32] D.-T. A. Pham, "Blind partial separation of instantaneous mixtures of sources," in *Proceedings of International Conference on Independent Component Analysis and Signal Separation*. Springer Berlin Heidelberg, 2006, pp. 868–875.
- [33] Z. Koldovský, P. Tichavský, and V. Kautský, "Orthogonally constrained independent component extraction: Blind MPDR beamforming," in *Proceedings of European Signal Processing Conference*, Sep. 2017, pp. 1195–1199.
- [34] J. F. Cardoso, "On extracting the cosmic microwave background from multi-channel measurements," in *Proceedings of International Conference on Latent Variable Analysis and Signal Separation*, Feb 2017, pp. 403–413.

- [35] J. F. Cardoso, M. L. Jeune, J. Delabrouille, M. Betoule, and G. Patanchon, "Component separation with flexible models - application to multichannel astrophysical observations," *IEEE Journal of Selected Topics in Signal Processing*, vol. 2, no. 5, pp. 735–746, Oct 2008.
- [36] I. Lee, T. Kim, and T.-W. Lee, "Independent vector analysis for convolutive blind speech separation," in *Blind speech separation*. Springer, 2007, pp. 169–192.
- [37] T. Adali, M. Anderson, and G. S. Fu, "Diversity in independent component and vector analyses: Identifiability, algorithms, and applications in medical imaging," *IEEE Signal Processing Magazine*, vol. 31, no. 3, pp. 18–33, May 2014.
- [38] H. L. Van Trees, *Optimum Array Processing: Part IV of Detection, Estimation, and Modulation Theory*. John Wiley & Sons, Inc., 2002.
- [39] J. F. Cardoso, "Multidimensional independent component analysis," in *Proceedings of IEEE International Conference on Audio, Speech and Signal Processing*, vol. 4, May 1998, pp. 1941–1944 vol.4.
- [40] A. Hyvärinen and U. Köster, "FastISA: A fast fixed-point algorithm for independent subspace analysis," in *14th European symposium on artificial neural networks, (ESANN 2006)*, 2006.
- [41] K. Matsuoka and S. Nakashima, "Minimal distortion principle for blind source separation," in *Proceedings of International Conference on Independent Component Analysis and Signal Separation*, Dec. 2001, pp. 722–727.
- [42] N. Duong, E. Vincent, and R. Gribonval, "Under-determined reverberant audio source separation using a full-rank spatial covariance model," *IEEE Transactions on Audio, Speech, and Language Processing*, vol. 18, no. 7, pp. 1830–1840, 2010.
- [43] Z. Koldovský and F. Nesta, "Performance analysis of source image estimators in blind source separation," *IEEE Transactions on Signal Processing*, vol. 65, no. 16, pp. 4166–4176, Aug. 2017.
- [44] H. Sawada, R. Mukai, S. Araki, and S. Makino, "A robust and precise method for solving the permutation problem of frequency-domain blind source separation," *IEEE Transactions on Speech and Audio Processing*, vol. 12, no. 5, pp. 530–538, Sep. 2004.
- [45] D. T. Pham and P. Garat, "Blind separation of mixture of independent sources through a quasi-maximum likelihood approach," *IEEE Transactions on Signal Processing*, vol. 45, no. 7, pp. 1712–1725, Jul 1997.
- [46] D. H. Brandwood, "A complex gradient operator and its application in adaptive array theory," *Communications, Radar and Signal Processing, IEE Proceedings F*, vol. 130, no. 1, pp. 11–16, February 1983.
- [47] H. Li and T. Adali, "Complex-valued adaptive signal processing using nonlinear functions," *EURASIP Journal on Advances in Signal Processing*, vol. 2008, Feb 2008, Article ID 765615.
- [48] A. Bell and T. Sejnowski, "An information-maximization approach to blind separation and blind deconvolution," *Neural Computation*, vol. 7, no. 6, pp. 1129–1159, 1995.
- [49] S. Amari, A. Cichocki, and H. H. Yang, "A new learning algorithm for blind signal separation," in *Proceedings of Neural Information Processing Systems*, 1996, pp. 757–763.
- [50] J. F. Cardoso and B. H. Laheld, "Equivariant adaptive source separation," *IEEE Transactions on Signal Processing*, vol. 44, no. 12, pp. 3017–3030, Dec 1996.
- [51] D. Lahat and C. Jutten, "Joint independent subspace analysis using second-order statistics," *IEEE Transactions on Signal Processing*, vol. 64, no. 18, pp. 4891–4904, Sept 2016.
- [52] M. Anderson, G. S. Fu, R. Phlypo, and T. Adali, "Independent vector analysis: Identification conditions and performance bounds," *IEEE Transactions on Signal Processing*, vol. 62, no. 17, pp. 4399–4410, Sept 2014.
- [53] E. Bingham and A. Hyvärinen, "A fast fixed-point algorithm for independent component analysis of complex valued signals," *International Journal of Neural Systems*, vol. 10, no. 1, pp. 1–8, Feb. 2000.
- [54] S. C. Douglas and M. Gupta, "Scaled natural gradient algorithms for instantaneous and convolutive blind source separation," in *2007 IEEE International Conference on Acoustics, Speech and Signal Processing - ICASSP '07*, vol. 2, April 2007, pp. II-637–II-640.
- [55] F. Nesta and Z. Koldovský, "Supervised independent vector analysis through pilot dependent components," in *2017 IEEE International Conference on Acoustics, Speech and Signal Processing (ICASSP)*, March 2017, pp. 536–540.